Insertion of alkynes into zirconium–nitrogen bonds leading to 2,3-diazametallacyclopentenes. Generation and reactivity of $Cp_2Zr(N_2Ph_2)$ *

Patrick J. Walsh, Frederick J. Hollander and Robert G. Bergman

Department of Chemistry, University of California, Berkeley, CA 94720 (USA)

(Received February 5, 1991)

Abstract

Methyl η^2-1,2-diphenylhydrazido(1^-)zirconocene (**1**) has been synthesized from the monopotassium salt of 1,2-diphenylhydrazine and $Cp_2Zr(Me)(Cl)$. Heating **1** in THF causes extrusion of methane, generating the transient hydrazido complex $Cp_2Zr(N_2Ph_2)$ (**2**) which is trapped by solvent to yield the THF adduct $Cp_2Zr(N_2Ph_2)(THF)$ (**3**). The THF ligand of compound **3** was replaced with a variety of σ-donor ligands to form the ligated hydrazido complexes $Cp_2Zr(N_2Ph_2)(L)$ (L = pyridine) (**4**), PMe_3 (**5**), NCPh (**6**) and $CNCMe_3$ (**7**)). Compound **4** was characterized by X-ray diffraction. The THF adduct **3** also undergoes a reaction involving insertion of alkynes into one of its metal–nitrogen bonds. Thus, reaction of **3** with 2-butyne and 3-hexyne leads to zirconocene 2,3-diazametallacyclopentenes **8** and **9** respectively. The structure of these metallacycles was supported by an X-ray diffraction study of **8**. Compound **3** also reacted with phenylacetylene and acetophenone via deprotonation to furnish the η^2-hydrazido(1^-)acetylide (**10**) and enolate (**11**), respectively.

Introduction

Insertion of unsaturated carbon–carbon bonds into metal–heteroatom bonds allows unsymmetrical functionalization of alkenes and alkynes. Ideally, the resulting metal–carbon bond can be further elaborated leading to construction of relatively complex skeletons from simple precursors. However, despite the potential applications of this seemingly fundamental process, examples of insertion of these substrates into transition metal–nitrogen bonds are surprisingly scarce [1–3].

Zirconocene heterometallacyclopropanes which contain oxygen, nitrogen and sulfur are known. However, these also contain Zr–C bonds and insertions readily occur into this linkage [4]. One approach to this problem would be to investigate heterometallacyclopropanes that contained only zirconium–nitrogen bonds. We report here the generation of the transient η^2-1,2-diphenylhydrazido(2^-)zircono-

---

* Dedicated to Professor Akio Yamamoto upon his retirement from the Tokyo Institute of Technology and in honor of his numerous contributions to organometallic chemistry.

cene complex $Cp_2Zr(N_2Ph_2)$ (2) which undergoes insertions of alkynes into the Zr–N bond to provide diazametallacyclopentenes [49].

Results

Synthesis of the η^2-hydrazido(1$^-$) complex $Cp_2Zr(NPhNHPh)(Me)$

Addition of alkali metal amides MNR_2 to early transition metal halides has proven to be a simple and efficient method for the synthesis of transition metal amides [1]. Similarly, reactions of the related alkali hydrazido(1$^-$) compounds $MNRNR'_2$ with metal halides leads to transition metal hydrazido(1$^-$) complexes [5] although this methodology does not appear to have been widely utilized.

$$Cp_2Zr(Cl)(Me) + KNPhNHPh \xrightarrow[25\,°C]{toluene} \mathbf{1} + KCl \qquad (1)$$
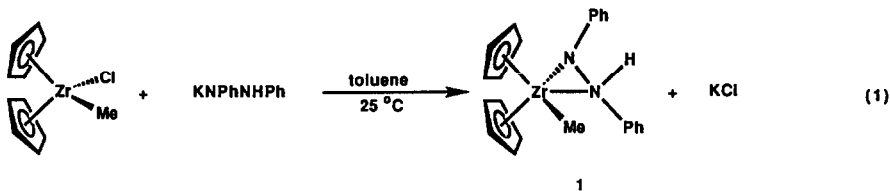
In our hands treatment of $Cp_2Zr(Me)(Cl)$ [6] with the monopotassium salt of 1,2-diphenylhydrazine in toluene (eq. 1) resulted in the formation of a fine precipitate (presumed to be KCl) and the zirconocene methyl hydrazido complex $Cp_2Zr(Me)(NPhNHPh)$ (1) which was isolated in 83% yield by crystallization from toluene layered with hexanes at $-30\,°C$. The η^2-hapticity of the hydrazido(1$^-$) ligand was apparent from ^1H and $^{13}C\{^1H\}$ NMR spectrometry; coordination of the β-nitrogen of the hydrazido ligand freezes the inversion at the nitrogen atom making the cyclopentadienyl ligands diasterotopic and chemically inequivalent. Thus the ^1H NMR spectrum of 1 (C_6D_6) contained resonances for the zirconium-bound methyl (0.04 ppm), an N–H (3.89 ppm), two inequivalent cyclopentadienyl ligands (5.46 and 5.60 ppm), and the expected aromatic resonances (6.55–7.24 ppm). The $^{13}C\{^1H\}$ NMR spectrum also contained resonances for the zirconium methyl (19.68 ppm), the inequivalent cyclopentadienyl ligands (108.75 and 110.01 ppm), and the aromatic carbons (113–157 ppm).

Synthesis of $Cp_2Zr(N_2Ph_2)(THF)$ and generation of the reactive intermediate $Cp_2Zr(N_2Ph_2)$

Our first evidence for the generation of $Cp_2Zr(N_2Ph_2)$ (2) was obtained by thermolysis of the η^2-hydrazido(methyl)zirconium complex 1 in THF-d_8 at 65°C for 2.5 d, which provided $Cp_2Zr(N_2Ph_2)(THF)$ (3) in 80% yield by ^1H NMR (eq. 2). Complex 3 was also prepared (60–80% yield) by addition of monolithio-1,2-diphenylhydrazine to $[Cp_2Zr(H)(Cl)]_n$ in THF (eq. 3), but it was obtained most efficiently (90–95% yield) and economically by the addition of Cp_2ZrCl_2 in THF to a solution of dilithio-1,2-diphenylhydrazide [7] in ether/THF at room temperature (eq. 4). Compound 3 prepared in this manner was consistently judged to be > 90% pure by ^1H NMR spectrometry and it was generally used without further purification. With great effort samples of 3 were crystallized from toluene at $-30\,°C$ for characterization by NMR spectrometry and elemental analysis. The ^1H NMR spectrum of 3 at room temperature, as well as other derivatives of 3 of the type $Cp_2Zr(N_2Ph_2)(L)$ (see Experimental), contain broad resonances owing to

reversible ligand dissociation and possibly to hindered rotation of the N-phenyl rings. Unfortunately, THF-d_8 was the only solvent in which **3** was both stable and soluble at the low temperatures required to slow the reversible loss of ligand and rotation of the N-phenyl groups. Owing to this difficulty the resonances of the bound THF were not observed by NMR because the THF ligand exchanged rapidly with the THF-d_8 solvent. The ^{1}H NMR spectrum of **3** at $-20\,^\circ$C in THF-d_8 contained resonances for two inequivalent cyclopentadienyl ligands (5.73 and 5.76 ppm) and resonances for two inequivalent phenyl groups, at least one of which is rotating slowly (or "frozen out") on the NMR time scale. At the same temperature the ^{13}C{^{1}H} NMR consists of two inequivalent cyclopentadienyl resonances (111.19 an 111.43 ppm), ten aromatic C–H signals (111–129 ppm) and two *ipso* carbons (161.15 and 163.22 ppm).

Ligand exchange reactions of $Cp_2Zr(N_2Ph_2)(THF)$

The coordinatively unsaturated intermediate **2** is most conveniently generated by dissociation of THF from adduct **3**. Thus, treatment of **3** with pyridine or

Table 1

Crystal and data collection parameters ^{a}

	4	**8**	**10**
Temperature (°C)	25	−108	−100
Empirical formula	$C_{27}H_{25}N_3Zr$	$C_{26}H_{26}N_2Zr$	$C_{30}H_{26}N_2Zr\cdot1/2C_7H_8$
Formula weight (amu)	482.7	457.7	545.8
Crystal size (mm)	$0.08\times0.25\times0.25$	$0.13\times0.15\times0.30$	$0.15\times0.15\times0.30$
Space group	*Pbca*	*Pna2$_1$*	*P2$_1$/n*
a (Å)	14.420(2)	17.6453(20)	7.766(3)
b (Å)	16.126(2)	8.2716(13)	22.493(4)
c (Å)	19.618(2)	29.181(10)	15.201(4)
α (°)	90.0	90.0	90.0
β (°)	90.0	90.0	97.04(3)
γ (°)	90.0	90.0	90.0
V (Å^3)	4561.9(18)	4259.1(25)	2636.9(21)
Z	8	8	4
d_{calc} (g cm^{-3})	1.41	1.43	1.37
μ_{calc} (cm^{-1})	4.9	5.2	4.3
Reflections measured	$+h,+k,+l$	$+h,+k,+l$	$+h,+k,\pm l$
Scan width	$\Delta\theta=0.55+0.35\tan\theta$	$\Delta\omega=0.60+0.35\tan\theta$	$\Delta\omega=0.85+0.35\tan\theta$
Scan speed (c, °/m)	$0.66\rightarrow6.70$	$0.72\rightarrow6.70$	4.02
Setting angles (2θ, °) ^{b}	24–24	24–24	24–28

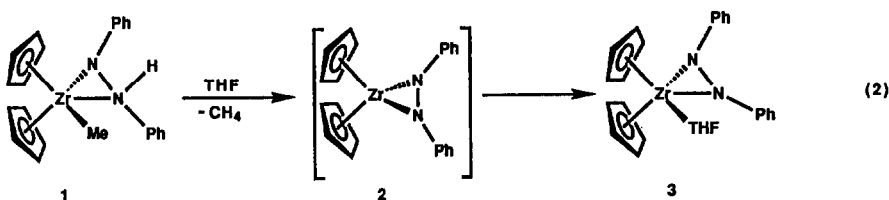^{a} Parameters common to all structures: Radiation: Mo-K_α (λ 0.71073 Å); monochromator: highly-oriented graphite ($2\theta=12.2\,°$); detector: crystal scintillation counter, with PHA; 2θ-range: $3\rightarrow45°$; scan type: for **4** $\theta-2\theta$, for **8** and **10** ω; background: measured over 0.25 ($\Delta\theta$) added to each end of the scan; vertical aperture = 3.0 mm except for **10** = 4.0 mm: horizontal aperture = $2.0+1.0\tan\theta$ mm except for **10** $2.5+1.0\tan\theta$ mm; intensity standards: measured every hour of X-ray exposure time; orientation: 3 reflections were checked after every 200 measurements; crystal orientation was redetermined if any of the reflections were offset from their predicted positions by more than 0.1°; reorientation was required twice for **4** and eight times for **8**. ^{b} Unit cell parameters and their esd's were derived by a least-squares fit to the setting angles of the unresolved Mo-K_α components of 24 reflections with the given 2θ-range. In this and all subsequent tables the esd's of all parameters are given in parentheses, right-justified to the least significant digit(s) of the reported value. ^{c} Angular velocity is for ϕ or ω depending on scan type.

Table 2

Selected intramolecular distances and esd's (Å) for complex **4**

Zr–N1	2.161(3)
Zr–N2	2.105(4)
Zr–N3	2.431(4)
Zr–C1	2.505(5)
Zr–C2	2.531(5)
Zr–C3	2.556(5)
Zr–C4	2.561(5)
Zr–C5	2.571(5)
Zr–Cp1	2.263
Zr–C6	2.543(4)
Zr–C7	2.526(5)
Zr–C8	2.529(5)
Zr–C9	2.525(5)
Zr–C10	2.549(5)
Zr–Cp2	2.246
N1–N2	1.434(4)
N1–C11	1.396(6)
N2–C17	1.368(6)
N3–C23	1.339(5)
N3–C27	1.324(5)
C23–C24	1.380(6)
C24–C25	1.375(7)
C25–C26	1.362(7)
C26–C27	1.383(7)
Phenyl C–C	1.368(6)–1.398(8)
Cyclopentadienyl C–C	1.348(8)–1.395(7)

trimethylphosphine led to complexes **4** and **5** in 72 and 83% isolated yield respectively (eq. 5). Compounds **4** and **5** exhibit fluxional behavior similar to that of **3** as indicated by ^{1}H and ^{13}C{^{1}H} NMR spectrometry. Crystals of the pyridine complex **4** suitable for an X-ray diffraction study were grown from a 50/50 mixture of toluene and hexanes at room temperature. Data collection parameters are given in Table 1 with bond distances, bond angles and torsional angles in Tables 2, 3 and 4 respectively. An ORTEP drawing of **4** is illustrated in Fig. 1. The structure consists of discrete molecules with no abnormally close intermolecular contacts. The N1–N2 bond length of 1.434(4) Å falls in the range of other known N–N single bonds [8]. Interestingly, N1 and N2 clearly are pyramidal, with a C_{ipso}–N1–N2–C_{ipso} torsional angle of 91.32(0.46)°. The zirconium–nitrogen bond lengths are 2.161(3) and 2.105(4) Å for the two anionic nitrogens and 2.431(4) Å for Zr–N3, the dative pyridine nitrogen [9,10].

(2)

$$\text{[Cp}_2\text{Zr(H)(Cl)]}_n \xrightarrow[\text{- LiCl}]{\text{LiNPhNHPh}} \left[\text{Zr} \begin{array}{c} \text{Ph} \\ \text{N} \\ \text{H} \end{array} \text{NHPh} \right] \xrightarrow[\text{- H}_2]{\text{THF}} \text{Zr} \quad \mathbf{3} \qquad (3)$$

$$\text{Cp}_2\text{ZrCl}_2 + \begin{array}{c} \text{Ph} \quad \text{Ph} \\ \text{N}-\text{N} \\ \text{Li} \quad \text{Li} \end{array} \xrightarrow[\text{- 2 LiCl}]{\text{THF/Et}_2\text{O}} \left[\mathbf{2} \right] \longrightarrow \mathbf{3} \qquad (4)$$

$$\mathbf{3} + \text{L} \xrightarrow{25\ ^\circ\text{C}} + \text{THF} \qquad (5)$$

4 L = Py
5 L = PMe₃
6 L = NCPh
7 L = CNCMe₃

$$\mathbf{3} + \text{RC}\equiv\text{CR} \xrightarrow{65\ ^\circ\text{C}} + \text{THF} \qquad (6)$$

8 R = Me
9 R = Et

$$\mathbf{1} + \text{EtC}\equiv\text{CEt} \xrightarrow{85\ ^\circ\text{C}} \mathbf{9} + \text{CH}_4 \qquad (7)$$
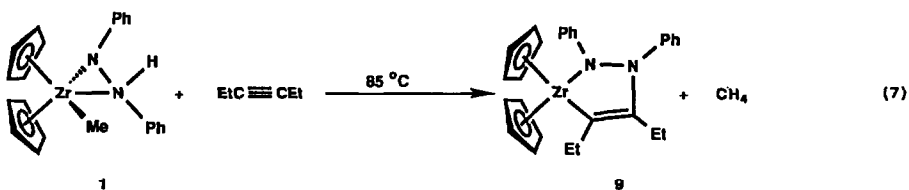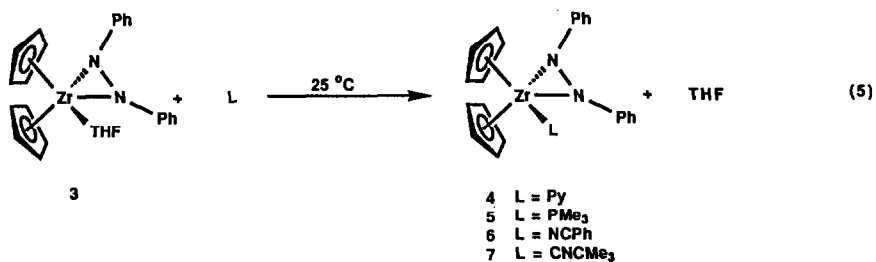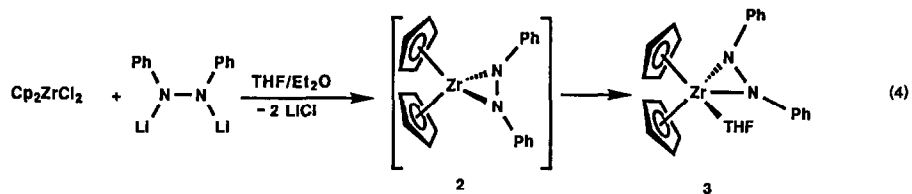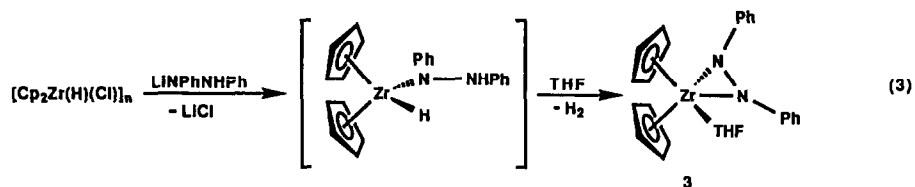
Table 3

Intramolecular bond angles (°) and esd's for complex 4

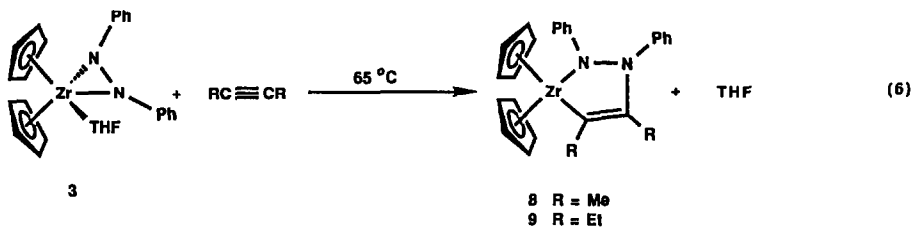| N1–Zr–N2	39.25(12)
N1–Zr–N3	118.75(13)
N2–Zr–N3	80.61(13)
N1–Zr–Cp1	106.1
N1–Zr–Cp2	104.6
N2–Zr–Cp1	123.3
N2–Zr–Cp2	108.0
N3–Zr–Cp1	97.5
N3–Zr–Cp2	104.4
Cp1–Zr–Cp2	126.7
Zr–N1–N2	68.3(2)
Zr–N1–C11	132.5(3)
Zr–N2–N1	72.5(2)
Zr–N2–C17	142.6(3)
C11–N1–N2	114.6(4)
C17–N2–N1	116.2(4)
N1–C11–C12	123.4(5)
N1–C11–C16	119.1(5)
N2–C17–C18	122.2(5)
N2–C17–C22	120.2(4)
Zr–N3–C23	117.5(3)
Zr–N3–C27	125.5(3)
C23–N3–C27	116.9(4)
N3–C23–C24	123.3(5)
N3–C27–C26	122.8(5)
C23–C24–C25	119.1(5)
C24–C25–C26	117.8(5)
C25–C26–C27	120.1(5)
Phenyl C–C–C	117.4(5)–121.8(6)
Cyclopentadienyl C–C–C	107.5(6)–108.7(5)

Nitriles have been observed to insert into group IV metal–nitrogen bonds to give η^2-amidino complexes [11]. In the case of 2, however, neither nitriles nor isonitriles undergo insertion into the M–N bonds. Thus, addition of 2.0 equivalents of t-butylisonitrile or benzonitrile to 2 in toluene leads to rapid formation of the complexes $Cp_2Zr(N_2Ph_2)(L)$ (6; L = NCPh; 7, L = CN^tBu) in 78 and 69% yield, respectively (eq. 5). The IR spectra of these complexes exhibit absorptions at 2256 and 2200 cm^{-1}, consistent with their assignment as coordination complexes rather than insertion products [11,12].

Reactions of $Cp_2Zr(N_2Ph_2)(THF)$ with internal alkynes

In contrast to known transition metal amides [1], internal alkynes react with THF complex 3 to give clean Zr–N insertion reactions. Thus, heating 3 at 45°C for 2 d in toluene in the presence of 4 equivalents of 2-butyne leads to a new complex 8 in 78% recrystallized yield in which the alkyne has been incorporated (eq. 6). The room temperature ^1H NMR spectra of 8 contained a single sharp resonance for the cyclopentadienyl ligands and two singlets for the methyl groups, but the phenyl region contained several broad absorptions. Cooling the sample in

Table 4

Torsional angles (°) and esd's for complex **4**

Zr–N1–N2	C17	− 140.58(0.35)
C11–N1–N2	Zr	− 128.09(0.34)
C11–N1–N2	C17	91.32(0.46)
Zr–N1–C11	C12	− 90.23(0.56)
Zr–N1–C11	C16	93.26(0.48)
N2–N1–C11	C12	− 7.83(0.62)
N2–N1–C11	C16	175.66(0.39)
Zr–N2–C17	C18	− 114.85(0.51)
Zr–N2–C17	C22	66.89(0.65)
N1–N2–C17	C18	− 19.66(0.60)
N1–N2–C17	C22	162.08(0.41)
N1–Zr–N3	C23	− 29.20(0.39)
N1–Zr–N3	C27	153.56(0.39)
N2–Zr–N3	C23	− 38.78(0.35)
N2–Zr–N3	C27	143.98(0.43)
Zr–N3–C23	C24	− 178.52(0.41)
C27–N3–C23	C24	− 1.04(0.76)
Zr–N3–C27	C26	− 179.86(0.45)
C23–N3–C27	C26	2.89(0.79)

CD_2Cl_2 resulted in initial broadening of the cyclopentadienyl resonance, followed by a split into two sharp signals at − 40 °C at 5.83 and 5.98 ppm. This inequivalence of the cyclopentadienyl ligands could be caused by slow loss of rotation of one of the phenyl rings or possibly by slow inversion of a puckered metallacycle
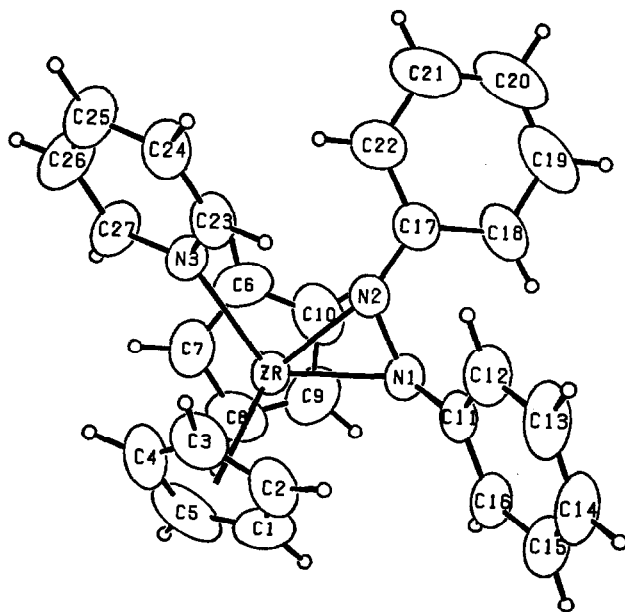

Fig. 1. Geometry and labeling scheme for **4**. The ellipsoids are scaled to represent the 50% probability surface.

Table 5

Selected intramolecular distances and esd's (Å) for molecule 1 of complex **8**

Zr1–N1	2.099(4)
Zr1–C2	2.257(5)
Zr1–C51	2.542(5)
Zr1–C52	2.509(5)
Zr1–C53	2.498(5)
Zr1–C54	2.520(5)
Zr1–C55	2.516(5)
Zr1–Cp1	2.217
Zr1–C56	2.518(5)
Zr1–C57	2.545(5)
Zr1–C58	2.543(5)
Zr1–C59	2.539(5)
Zr1–C60	2.528(5)
Zr1–Cp2	2.236
N1–N2	1.433(6)
N2–C1	1.442(7)
C1–C2	1.325(7)
N1–C11	1.400(6)
N2–C21	1.410(7)
C1–C3	1.515(8)
C2–C4	1.531(8)
Phenyl C–C	1.364(8)–1.401(7)
Cyclopentadienyl C–C	1.384(8)–1.435(8)

Table 6

Intramolecular bond angles (°) and esd's for molecule 1 of complex **8**

Cp1–Zr1–N1	106.99
Cp2–Zr1–N1	117.85
Cp1–Zr1–C2	106.93
Cp2–Zr1–C2	106.09
Cp1–Zr1–Cp2	127.17
N1–Zr1–C2	81.35(18)
Zr1–N1–N2	93.0(3)
N1–N2–C1	118.2(4)
N2–C1–C2	115.2(5)
C1–C2–Zr1	102.9(4)
Zr1–N1–C11	143.4(4)
N2–N1–C11	114.8(4)
N1–N2–C21	116.5(4)
C1–N2–C21	125.2(4)
N2–C1–C3	116.2(5)
C2–C1–C3	128.5(5)
Zr1–C2–C4	136.7(4)
C1–C2–C4	120.2(5)
N1–C11–C12	123.4(5)
N1–C11–C16	118.9(5)
N2–C21–C22	120.2(4)
N2–C21–C26	120.8(5)
Phenyl C–C–C	117.7(5)–120.5(6)
Cyclopentadienyl C–C–C	107.4(5)–109.1(5)

Table 7

Torsional angles (°) and esd's for molecule 1 and 2 of complex **8**

Molecule 1	
C2–Zr1–N1–N2	− 39.44(0.27)
C2–Zr1–N1–C11	101.24(0.57)
Cp1–Zr1–N1–N2	− 144.60
Cp1–Zr1–N1–C11	− 3.93
Cp2–Zr1–N1–N2	64.25
Cp2–Zr1–N1–C11	− 155.07
N1–Zr1–C2–C1	23.96(0.34)
N1–Zr1–C2–C4	− 150.99(0.53)
Cp1–Zr1–C2–C1	129.19
Cp1–Zr1–C2–C4	− 45.76
Cp2–Zr1–C2–C1	− 92.65
Cp2–Zr1–C2–C4	92.40
Zr1–N1–N2–C1	58.67(0.41)
Zr1–N1–N2–C21	− 117.71(0.37)
C11–N1–N2–C1	− 96.72(0.48)
C11–N1–N2–C21	86.90(0.51)
Zr1–N1–C11–C12	− 111.56(0.59)
Zr1–N1–C11–C16	67.06(0.73)
N2–N1–C11–C12	24.26(0.64)
N2–N1–C11–C16	− 157.11(0.44)
N1–N2–C1–C2	− 44.61(0.62)
N1–N2–C1–C3	132.67(0.45)
C21–N2–C1–C2	131.42(0.52)
C21–N2–C1–C3	− 15.30(0.67)
N1–N2–C21–C22	− 11.52(0.67)
N1–N2–C21–C26	164.70(0.45)
C1–N2–C21–C22	172.39(0.47)
C1–N2–C21–C26	− 11.39(0.76)
N2–C1–C2–Zr1	1.10(0.51)
N2–C1–C2–C4	177.09(0.44)
C3–C1–C2–Zr1	− 175.78(0.46)
C3–C1–C2–C4	0.21(0.83)
Molecule 2	
C6–Zr2–N3–N4	33.96(0.26)
C6–Zr2–N3–C31	− 11.71(0.54)
Cp4–Zr2–N3–N4	136.55
Cp4–Zr2–N3–C31	− 9.12
Cp3–Zr2–N3–N4	− 70.66
Cp3–Zr2–N3–C31	143.68
N3–Zr2–C6–C5	− 18.21(0.33)
N3–Zr2–C6–C8	156.58(0.53)
Cp4–Zr2–C6–C5	− 126.42
Cp4–Zr2–C6–C8	48.37
Cp3–Zr2–C6–C5	95.46
Cp3–Zr2–C6–C8	− 89.75
Zr2–N3–N4–C5	− 51.86(0.38)
Zr2–N3–N4–C41	117.62(0.34)
C31–N3–N4–C5	106.06(0.45)
C31–N3–N4–C41	− 84.46(0.48)
Zr2–N3–C31–C32	129.64(0.50)
Zr2–N3–C31–C36	− 48.60(0.74)

Table 7 (continued)

Molecule 2	
N4–N3–C31–C32	– 12.39(0.64)
N4–N3–C31–C36	169.38(0.42)
N3–N4–C5–C6	42.02(0.58)
N3–N4–C5–c7	– 132.09(0.43)
C41–N4–C5–C6	– 127.22(0.47)
C41–N4–C5–C7	58.67(0.56)
N3–N4–C41–C42	19.40(0.60)
N3–N4–C41–C46	– 159.61(0.41)
C5–N4–C41–C42	– 171.33(0.41)
C5–N4–C41–C46	9.66(0.63)
N4–C5–C6–Zr2	– 4.33(0.48)
N4–C5–C6–C8	179.93(0.43)
C7–C5–C6–Zr2	169.06(0.41)
C7–C5–C6–C8	– 6.67(0.79)

[13]. The most informative feature in the $^{13}C\{^1H\}$ NMR spectrum was the quaternary carbon signal at 172.34 ppm which falls in the range normal for sp^2-hybridized carbons bound to the Cp_2Zr moiety [14]. These data support the proposed 2,3-diazametallacyclopentene structure of **8** shown in eq. 6. In analogy to the preparation of **8**, heating THF adduct **3** with 3-hexyne to 45 °C for 5 d resulted in the formation of the metallacycle **9** which was isolated in 91% yield. Compound **9**
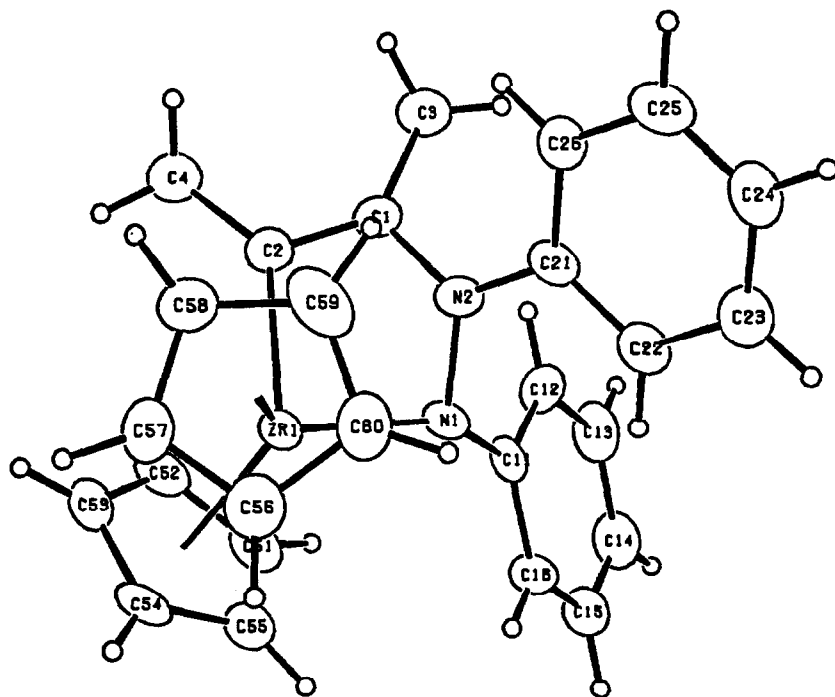

Fig. 2. Geometry and labeling scheme for molecule **1** of **8**. The ellipsoids are scaled to represent the 50% probability surface. Hydrogen atoms are given as arbitrarily small spheres for clarity.

crystallized from ether contained one molecule of solvent per two zirconium atoms in the crystal lattice, and exhibited spectroscopic characteristics similar to those of **8**. Metallacycle **9** was independently generated by the thermolysis of $Cp_2Zr(NPhNHPh)(Me)$ in C_6D_6 in 89% yield (^1H NMR) as illustrated in eq. 7.

Crystals of **8** were grown from a toluene/hexane solution at room temperature and X-ray data were collected at $-108°C$. The structure was solved by standard least-squares and Fourier techniques. Data collection parameters are listed in Table 1 with bond lengths, bond angles and torsional angles in Tables 5, 6 and 7 respectively. The ORTEP drawing shown in Fig. 2 illustrates the metallacyclic nature of **8**. Compound **8** crystallizes in the space group $Pna2_1$ with 2 independent molecules in the crystallographic asymmetric unit. The molecules are very similar, with small but significant differences in torsional angles around certain bonds (Table 7). Although there are some marginal differences in bond lengths (*e.g.*, in the Zr–N bond) these should be discounted owing to the low (4.86/1) data to parameter ratio. The normal underestimation of these esd's using errors generated in the least-squares refinement is aggravated by such a ratio.

As suggested by the variable temperature NMR spectra, the 2,3-diazametalla-cyclopentene does exist in an envelope configuration in the solid state, with a clearly localized C–C double bond of 1.333(7) and a N–N distance of 1.431(6) Å (bond lengths in the text are given as an average of the two asymmetric molecules). The Zr–N and Zr–C bond distances of 2.108(4) and 2.250(5) Å are typical for

Table 8

Selected intramolecular distances and esd's (Å) for complex **10** [a]

Zr	N1	2.344(4)
Zr	N2	2.122(5)
Zr	C13	2.258(6)
Zr	C21	2.548(6)
Zr	C22	2.513(6)
Zr	C23	2.521(6)
Zr	C24	2.558(60
Zr	C25	2.535(6)
Zr	C26	2.516(7)
Zr	C27	2.526(6)
Zr	C28	2.538(6)
Zr	C29	2.529(6)
Zr	C30	2.491(7)
N1	N2	1.410(6)
N1	C1	1.437(7)
N2	C7	1.385(7)
C13	C14	1.208(8)
C14	C15	1.454(9)
C31	C32	1.373(4)
C31	C33	1.415(12)
C32	C33	1.419(13)
C33	C34	1.217(16)
Phenyl C–C		1.373(9)–1.398(8)
Cyclopentadienyl C–C		1.383(9)–1.410(9)

[a] Atoms C31–C34 refer to the disordered toluene solvate (not illustrated).

Table 9

Intramolecular bond angles (°) and esd's for complex **10** [a]

N1–Zr–N2	36.38(15)
N1–Zr–C13	80.33(18)
N1–Zr–C21	118.59(210
N1–Zr–C22	149.16(20)
N1–Zr–C23	137.84(20)
N1–Zr–C24	106.91(18)
N1–Zr–C25	97.38(19)
N1–Zr–C26	80.29(22)
N1–Zr–C27	82.35(19)
N1–Zr–C28	112.95(19)
N1–Zr–C29	132.13(19)
N1–Zr–C30	109.13(24)
N2–Zr–C13	115.41(19)
N2–Zr–C21	117.24(22)
N2–Zr–C22	131.95(20)
N2–Zr–C23	105.16(21)
N2–Zr–C24	79.08(19)
N2–Zr–C25	85.93(20)
N2–Zr–C26	77.25(21)
N2–Zr–C27	97.66(21)
N2–Zr–C28	128.41(20)
N2–Zr–C29	124.73(20)
N2–Zr–C30	92.74(24)
C13–Zr–C21	74.92(21)
C13–Zr–C22	92.80(22)
C13–Zr–C23	124.68(22)
C13–Zr–C24	124.32(21)
C13–Zr–C25	93.26(22)
C13–Zr–C26	111.1(3)
C13–Zr–C27	79.94(24)
C13–Zr–C28	76.64(22)
C13–Zr–C29	104.83(23)
C13–Zr–C30	128.79(24)
N2–N1–C1	119.3(4)
N1–N2–C7	117.7(5)
N1–C1–C2	117.4(5)
N1–C1–C6	121.7(5)
N2–C7–C8	123.9(5)
N2–C7–C12	118.0(6)
C13–C14–C15	179.0(7)
C14–C15–C16	120.7(6)
C14–C15–C20	121.4(6)
C31–C32–C33	120.8(10)
C31–C33–C32	119.8(10)
C31–C33–C34	120.3(13)
C32–C33–C34	119.8(12)
Phenyl C–C–C	117.8(5)–121.6(6)
Cyclopentadienyl C–C–C	107.5(6)–108.5(7)

[a] Atoms C31–C34 refer to the toluene solvate (not illustrated).

bonds between these elements [9]. The nitrogen atom N1 has a pyramidal geometry while N2 is almost planar.

Reaction of Cp$_2$Zr(N$_2$Ph$_2$)(THF) with acidic C–H bonds

Group 4 metal amide complexes react with weakly acidic protons to liberate amine [15]. We have observed analogous reactivity with the hydrazido(2⁻) ligand. Phenylacetylene reacted with **3** to give a new product which exhibited an NH stretch in the IR at 3205 cm^{-1} (eq. 8). This material was isolated in 64% recrystallized yield and is formulated as the η^2-hydrazido(1⁻) acetylide complex **10**. However no absorption attributable to a C–C triple bond was observed in the IR and a resonance characteristic of the α-carbon of the acetylide ligand was not
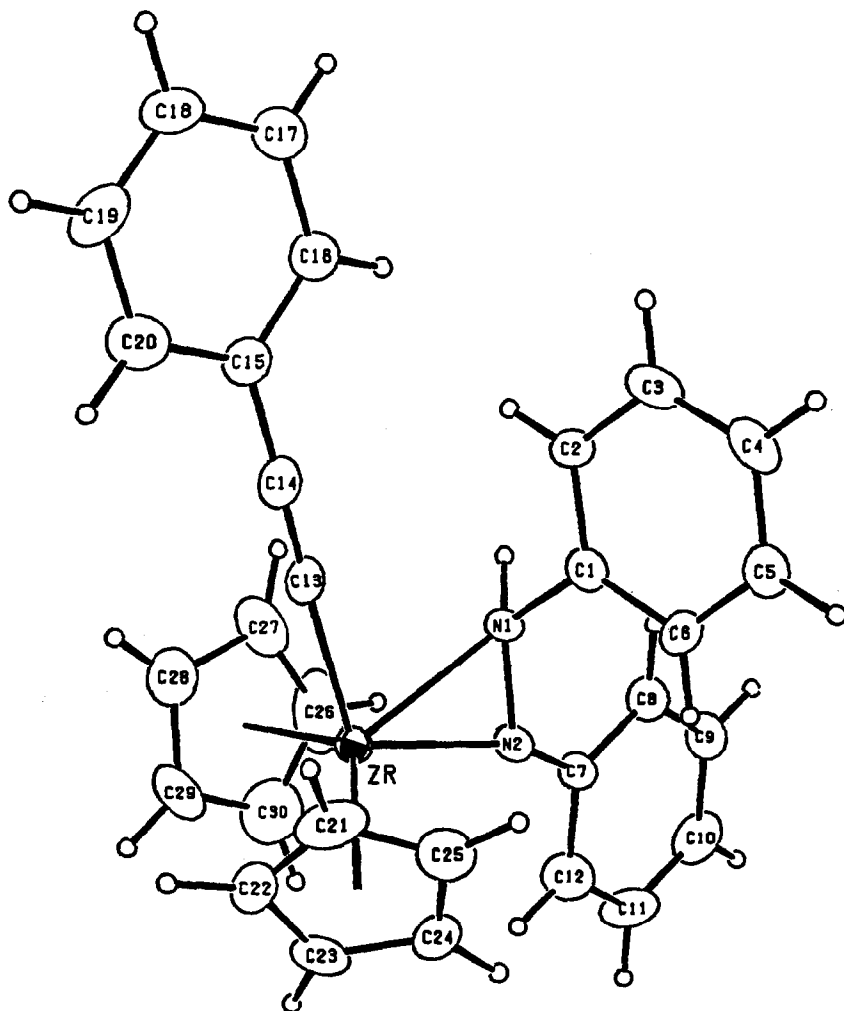

Fig. 3. Geometry and labeling scheme for **10**. The ellipsoids are scaled to represent the 50% probability surface. Hydrogen atoms are given as arbitrarily small spheres for clarity.

located in the $^{13}C\{^1H\}$ NMR despite a search over various temperatures and solvents [16]. For these reasons an X-ray structural study of **10** was undertaken to confirm the proposed connectivity. Yellow crystals of **10** grown from toluene layered with pentane at $-30°C$ crystallized in the space group $P2_1/n$ and data were collected at $-100°C$. The structure was solved by Patterson methods and refined via standard least-squares and Fourier techniques. Data collection parameters are listed in Table 1 with bond distances and bond angles in Tables 8 and 9, respectively. An ORTEP diagram is illustrated in Fig. 3. The structure consists of discrete molecular units with no abnormally close contacts. The hydrazido(1^-) ligand is bonded in the η^2-fashion with a dative bond between N1 and Zr with the tetrahedral N1 occupying the less sterically demanding central position of the wedge. The Zr–N1 and Zr–N2 bond lengths of 2.344(4) and 2.122(5) Å fall in the range of dative and σ-nitrogen bonded to zirconium [9,10] respectively. The Zr–C bond length of 2.258(6) Å compares with the value found for $Cp_2Zr(CCMe)_2$ of 2.249(3) Å [16]. The phenyl acetylide ligand (Zr–C–C) is nearly linear at 179.0(7)°. The C13–C14 distance of 1.208(8) Å is typical for σ-bonded acetylides and, as observed by Erker *et al.,* is close to the distance observed in free alkynes and acetylides of main group metals [16].
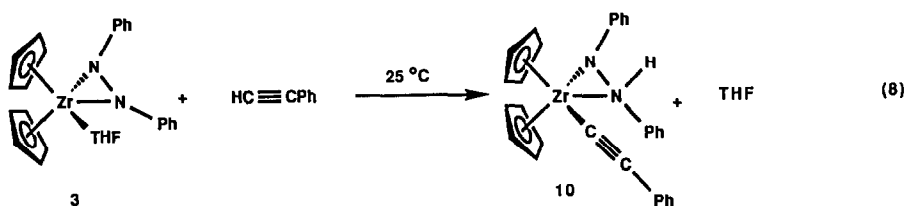
Acetophenone reacted with **3** in a similar manner to give enolate **11**, which was isolated in 67% recrystallized yield (eq. 9). Complex **11** exhibited an NH stretch in the IR at 3220 and a strong absorption at 1591 cm^{-1} [17]. The ^1H NMR spectrum (C_6D_6) of **11** contained singlets at 4.05, 4.65, 4.78, 5.87, and 6.00 ppm in a ratio of 1/1/1/5/5 as well as the aromatic resonances from 6.66–7.41 ppm integrating to 15 protons. These data are consistent with the η^2-hydrazido(1^-) O-bound enolate structure illustrated in eq. 9 where the resonances are the two inequivalent CH's of the enolate, the N–H and the protons of the cyclopentadienyl ligands which are inequivalent owing to the η^2-hapticity of the hydrazido(1^-) ligand. Further support for the proposed structure of complex **11** was the resonance for the methylene carbon of the enolate in the $^{13}C\{^1H\}$ NMR at 82.21 ppm in THF-d_8 [18].
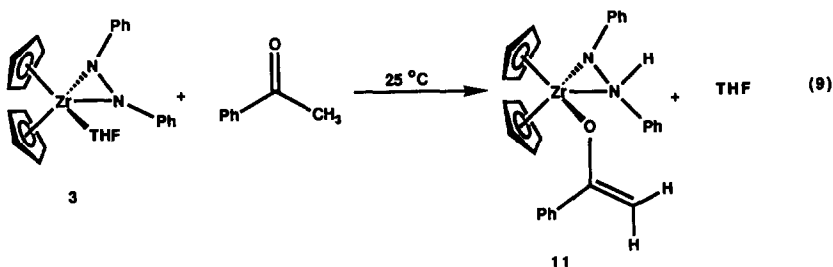
Discussion

Design of system

In our search for early metal systems which might undergo insertion of molecules containing unsaturated C–C bonds, the class of compounds of the type $Cp_2Zr(X-Y)$ appear particularly interesting. These species, which cannot usually be isolated, have been trapped as their ligand adducts $Cp_2Zr(X-Y)(L)$ or by dimerization to give $[Cp_2Zr(X-Y)]_2$. One example of a complex of this type is the zirconium benzyne complex $Cp_2Zr(C_6H_4)$ [19] which can be generated from thermolysis of $Cp_2Zr(Ph)_2$ or by loss of phosphine from the ligand adduct $Cp_2Zr(C_6H_4)(PMe_3)$ [20]. The benzyne complex $Cp_2Zr(C_6H_4)$ readily undergoes insertion of olefins and alkynes into a Zr–C bond to give the corresponding 5-membered metallacycle.
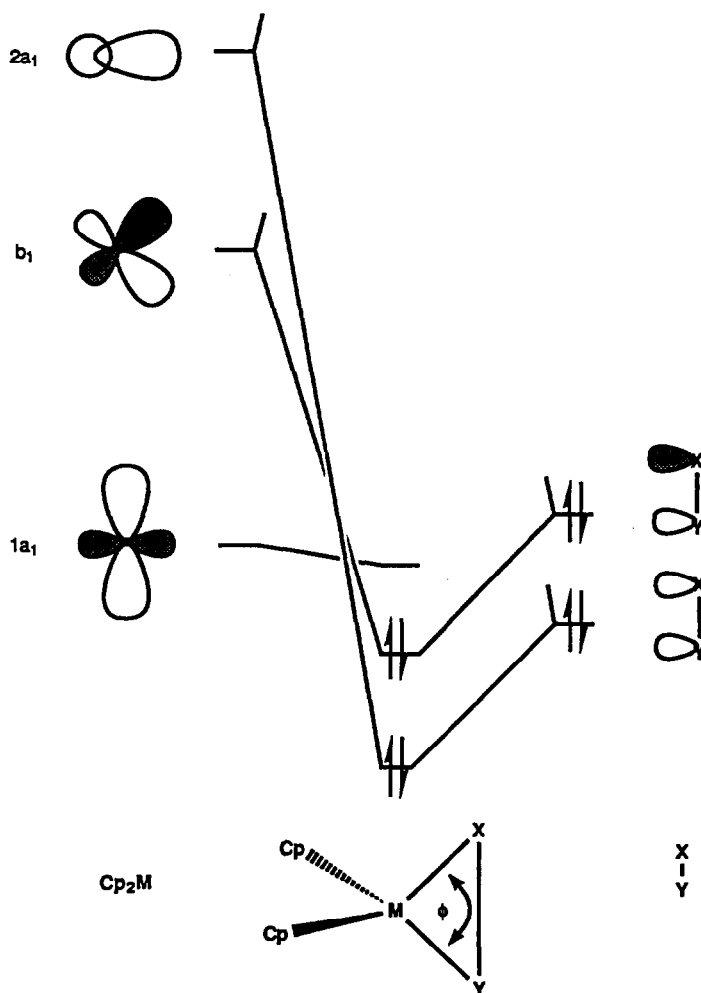

Fig. 4. Interaction diagram illustrating combination of the combination of generally accepted orbitals of the Cp_2M^{2+} fragment (left) with the dianion X–Y.

Related examples containing heteroatoms include the η^2-benzophenone complex $Cp_2Zr(OCPh_2)$ [4a], the η^2-imine complex $CP_2Zr(NR–CHR')$ [4b,c] and the η^2-thioaldehyde complex $Cp_2Zr(S–CHR)$ [4e,f]. These complexes, which all have transient existence, are very reactive and undergo insertion of olefins and alkynes to give heterometallacycles. However, in all cases the unsaturated group inserts into the Zr–C bond. The η^2-benzophenone complex reacts even with toluene at the Zr–C bond to provide the C–H activation product $Cp_2Zr(OCHPh_2)(Tol)$ [3a]. Because of this favorable insertion into M–C bonds, we chose to work with a $Cp_2Zr(X–Y)$ system in which both X and Y are heteroatoms, and this led us to examine the chemistry of the η^2-hydrazido(2$^-$) complex $Cp_2Zr(N_2Ph_2)$.

Our explanation for the reactivity of the complexes $Cp_2Zr(X–Y)$ is based on molecular orbital theory. Extensive experimental and theoretical work [21] has been performed on the electronic structure of bent metallocene systems. The generally accepted frontier orbitals for the bent Cp_2M fragment are illustrated on the left of Fig. 4.

One particularly interesting prediction concerns the angle ϕ (X–M–Y) between two groups X and Y in the compounds $Cp_2M(X)(Y)$. In compounds of this type it has been suggested that the energies of the a_1 orbitals are very sensitive to the angle ϕ (Fig. 4) [21a,c]. More specifically, calculations by Lauher and Hoffmann predict that at relatively large values of ϕ, overlap of the σ-donating orbitals of X and Y with the $1a_1$ and the $2a_1$ fragment orbitals is large, and this produces a large splitting in the resulting interaction orbitals. As the angle ϕ decreases the interaction of the ligands with the $1a_1$ orbital decreases until $\phi = \sim 78°$ where the M–X and M–Y bonds lie approximately on the nodes of the $1a_1$ orbital. As ϕ continues to decrease a plot of the energy of the a_1 orbitals vs. ϕ indicates a sharp increase in the energy of the a_1 orbitals as ϕ becomes less than $\sim 70°$ [21a]. For both steric and electronic reasons ϕ is expected to remain $> 70°$ in conventional $Cp_2M(X)(Y)$ compounds. However, by linking together the ligands X and Y with a bond, ϕ is restricted to values substantially lower than those achievable in the $Cp_2M(X)(Y)$ system. We believe that this has two consequences: (i) the increase in energy of the a_1 orbitals caused by small values of ϕ ($\sim 40°$) will result in a decrease in the net stabilization gained through interaction of the ligands X and Y with the metal orbitals and will therefore weaken the M–X and M–Y bonds; (ii) the steric environment at the metal center will be reduced, facilitating coordination of additional ligands which can react further with the M–X or M–Y bonds.

Synthesis and thermal decomposition of Cp₂Zr(Me)(NPhNHPh)

The generation of metallacyclopropanes and heterometallacyclopropanes by β-extrusion of an alkane or arene has been particularly successful in a number of systems involving the Cp_2Zr moiety. However, in the cases studied the elimination of alkane or arene has resulted in formation of an M–C bond. Application of this methodology to the generation of η^2-hydrazido(2$^-$) complex $Cp_2Zr(N_2Ph_2)$ (2) from $Cp_2Zr(Me)(NPhNHPh)$ requires breaking an N–H bond.

The synthesis of the methyl η^2-hydrazido(1$^-$) complex $Cp_2Zr(Me)(NPhNHPh)$ (1) illustrated in eq. 1 was similar to our earlier preparation of analogous alkyl amides of the type $Cp_2Zr(NHR)(Me)$ [6b]. η^1-Coordination of the hydrazido(1$^-$) ligand of 1 [22] would leave the zirconium center with formally 16 electrons and thus an open coordination site. However, the metal can achieve an 18-electron

configuration by dative coordination of the β-nitrogen of the hydrazido(1$^-$) ligand. The η^2-hapticity of the hydrazido(1$^-$) ligand was evident from ^{1}H and ^{13}C{^{1}H} NMR spectrometry, which indicated that the cyclopentadienyl ligands were inequivalent owing to coordination of the β-nitrogen of the hydrazido ligand to the zirconium.

Thermolysis of **1** in THF-d_8 resulted in the formation of methane and the η^2-hydrazido(2$^-$) complex Cp$_2$Zr(N$_2$Ph$_2$)(THF) (**3**) in 80% yield. This product presumably arises via β-extrusion of methane from **1** through a four-center transition state [4e,23] to generate the transient species Cp$_2$Zr(N$_2$Ph$_2$) which is rapidly trapped by the THF solvent (eq. 2). It is interesting to note that in spite of its somewhat higher acidity, the nitrogen-bound β-hydrogen in **3** is not eliminated substantially faster than the carbon-bound β-hydrogens in Cp$_2$ZrPh$_2$ [19,20]. Cp$_2$Zr(NSiR$_3$CH$_2$Ph)(R) [4b,c], and Cp$_2$Zr(SCH$_2$R)(R) [4e,f]. However, the elimination of methane from **1** is complicated by the hapticity of the hydrazido ligand. It is possible that the rate-determining step in the generation of the transient Cp$_2$Zr(N$_2$Ph$_2$) could involve η^2-to-η^1 isomerization of the hydrazido(1$^-$) ligand before methane is extruded.

Although the synthesis of **3** from Cp$_2$ZrCl$_2$ via Cp$_2$Zr(NPhNHPh)(Me) proceeds in good yield, it requires four steps and so we sought a more direct route. In one alternative procedure, we found that **3** could be prepared from the commercially available polymeric [Cp$_2$Zr(H)(Cl)]$_n$ and the monolithium salt of 1,2-diphenylhydrazine in THF in 60–80% yield as illustrated in eq. 3. This transformation most likely involves initial nucleophilic displacement of the chloride to give the intermediate hydrido hydrazido(1$^-$) complex Cp$_2$Zr(H)(NPhNHPh). This then loses H$_2$ to generate **2**, which reacts rapidly with THF. While this method is more efficient than the route starting from Cp$_2$Zr(Me)(NPhNHPh), the resulting Cp$_2$Zr-(N$_2$Ph$_2$)(THF) contains unidentified contaminants that are extremely difficult to remove. Therefore, a second alternative synthesis of **3** was worked out which involved the use of the dilithio salt of 1,2-diphenylhydrazine [7]. Addition of this dianion to Cp$_2$ZrCl$_2$ in THF resulted in the clean formation of Cp$_2$Zr(N$_2$Ph$_2$)-(THF) in 90–95% yield (eq. 4).

The transient intermediate Cp$_2$Zr(N$_2$Ph$_2$) (**2**) is readily regenerated from the THF adduct **3** at 25°C by reversible dissociation of the weakly bound THF ligand. Thus addition of the dative ligands pyridine or trimethylphosphine to **3** resulted in formation of the adducts Cp$_2$Zr(N$_2$Ph$_2$)(py) (**4**) and Cp$_2$Zr(N$_2$Ph$_2$)(PMe$_3$) (**5**) in 72 and 84% recrystallized yields, respectively (eq. 5). An X-ray diffraction study of **4** confirmed the proposed connectivity of the η^2-hydrazido(2$^-$) pyridine adduct; an ORTEP diagram is shown in Fig. 1 (see Results). The Zr–N bond lengths of the η^2-hydrazido(2$^-$) ligand of 2.161(3) and 2.105(4) Å are typical of Zr–N bond lengths in zirconium amides [9]. The constrained N1–Zr–N2 angle is 39.25(12)° and the N1–N2 bond length of 1.434(4) Å is clearly consistent with the presence of an N–N single bond [8]. Owing to the geometrical constraints of the 3-membered ZrN$_2$ ring, the bond distances and angles of the zirconium hydrazido(2$^-$) linkage are not expected to change greatly on going from the ligand adducts **3–5** to the unsaturated intermediate Cp$_2$Zr(N$_2$Ph$_2$) and the N–Zr–N angle ϕ is expected to remain small.

Insertion of polarized unsaturated organic molecules into Zr–N bonds generally occurs with a net change in hapticity between the initial amide and the insertion

product. For example, CO_2 inserts into group IV M−N bonds to give O,O-bound η^2-carbamates as determined by low values of $\nu(CO)$ (eq. 10) [24]. Similar reactivity and hapticity changes have been observed with other heterocumulenes [1b,24a,25]. Nitriles follow a similar trend, inserting into group IV metal amides to furnish η^2-amidino complexes [24a,26]. In contrast, addition of benzonitrile or t-butylisonitrile to **3** resulted only in the formation of dative ligand adducts $Cp_2Zr(N_2Ph_2)(NCPh)$ (**5**) and $Cp_2Zr(N_2Ph_2)(CNCMe_3)$ (**6**) (eq. 5). The presence of a coordinated nitrile in **5** results in an absorption at 2256 cm^{-1} in the IR spectrum, which is at higher frequency than that of the free nitrile (2231 cm^{-1}) [12,27,28]. This is consistent with a dominant σ-donor interaction, similar to that observed in other nitrile-Lewis acid adducts. Coordination of acetonitrile to Lewis acids such as BX_3 (X = F, Cl, Br) normally results in a shift to higher frequency (by > 100 cm^{-1}). In late metal nitrile complexes the shift of $\nu(CN)$ to lower frequency has normally been attributed to a decrease in the C−N bond order caused by back-donation of the d electrons from a filled metal orbital into a π^* orbital of the nitrile C−N bond.

$$Me_2Hf(N(SiMe_3)_2)_2 \quad + \quad CO_2 \quad \longrightarrow \quad Me_2Hf \overset{O}{\underset{O}{\diamond}} C\text{-}N(SiMe_3)_2 \quad (10)$$

Isonitriles are commonly used to stabilize low formal oxidation state metals. However, they also can act as σ-donors to Lewis acids. The IR stretch of **6** at 2200 cm^{-1} (CH_2Cl_2) is shifted to higher frequency relative to free t-butylisonitrile ($\nu(CN) = 2139$ cm^{-1} in CH_2Cl_2) [29]. Isonitriles are better σ-donors than nitriles. As in the nitrile case discussed above, the Zr−C σ interaction of the isonitrile is stronger than the $\pi^*/1a_1$ back-bonding and dominates the bonding as demonstrated by IR spectrometry. In contrast to the observations in our system, a decrease in $\nu(CO)$ was observed by Bercaw and co-workers in the coordination of CO to $Cp_2^*ZrH_2$ at low temperature [30], perhaps because of the better back-bonding ability of carbon monoxide or the increased donating capacity of $Cp_2^*ZrH_2$.

The insertion of internal alkynes into $Cp_2Zr(N_2Ph_2)$

Insertion of alkenes or alkynes into M−N bonds in metal amides results in functionalizing of the inserting group in an unsymmetrical fashion and leads to a new M−C bond which can potentially be further manipulated [31]. Realization of this process has been rare so far, but Gagné and Marks [3c] recently found that the lanthanide complex $[Cp_2^*LaH]_2$ catalyzes the cyclization of amino olefins to provide a number of 5 and 6-membered cyclic amines. Casalnuovo *et al.* [3d] have also designed an iridium catalyst which hydroaminates norbornene. However, less than 6 turnovers were observed before catalyst decomposition was complete. The proposed mechanism involves the insertion of norbornene into the Ir−N bond.

In the case of the η^2-hydrazido(2^-) complex **3**, mild heating in the presence of 2-butyne or 3-hexyne resulted in insertion of the alkyne into the metal−nitrogen bond to provide the 2,3-diazametallacyclopentenes **8** and **9** in 78 and 91% recrystallized yield (eq. 6). Metallacycle **9** was also formed in 91% yield by heating **1** and 3-hexyne (eq. 7). Formation of this product from **3** most likely arises from loss of ligand to generate the unsaturated $Cp_2Zr(N_2Ph_2)$ which undergoes coordination
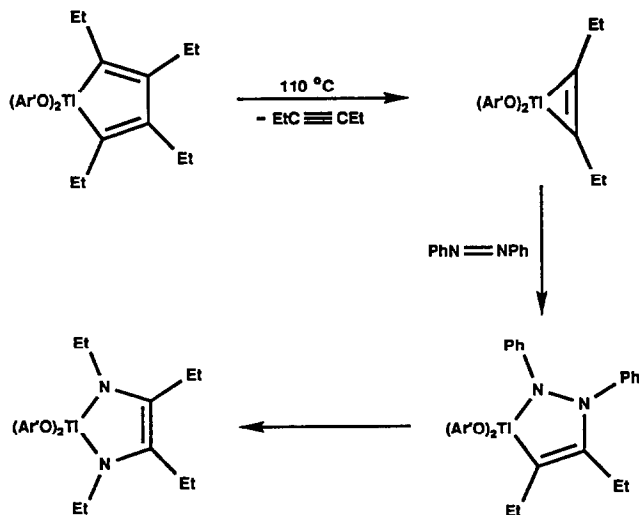
Scheme 1

of alkyne followed by migratory insertion to form the observed product. An ORTEP diagram illustrating the structure of **8** is shown in Fig. 2.

Recently, 2,3-diazametallacyclopentenes analogous to **8** and **9** were proposed as intermediates in the titanium mediated N–N bond cleavage of azobenzene shown in Scheme 1 [32]. However, no such reactivity of metallacycle **9** was observed. Heating **9** to 85°C for 24 h led only to decomposition.

There are not many other reactions of η^2-hydrazido(2$^-$) complexes with which our results can be compared. Floriani and his co-workers have prepared the η^2-hydrazido(2$^-$) complexes $Cp_2Ti(N_2Ph_2)$ [33] and $Cp_2V(N_2Ph_2)$ [34] by treatment of azobenzene with $Cp_2Ti(CO)_2$ and Cp_2V, respectively [35*]. The molybdenum analogue $Cp_2Mo(N_2Ph_2)$ was prepared by Otsuka et al. by the addition of 2 equivalents of azobenzene to Cp_2MoH_2 with generation of an equivalent of 1,2-diphenylhydrazine [36].

The structure of $Cp_2Ti(N_2Ph_2)$ [37] is significantly different from that of the zirconium η^2-hydrazido(2$^-$) $Cp_2Zr(N_2Ph_2)(py)$. Most noticeably, the 16-electron titanium complex does not coordinate an additional ligand. The different coordination number of these hydrazido(2$^-$) complexes may be ascribed to the difference in ionic radius between titanium and zirconium. The Ti and Zr complexes also exhibit a substantial difference in the N–N bond lengths. The N–N bond distance in $Cp_2Ti(N_2Ph_2)$ of 1.338(9) Å is significantly shorter than that in $Cp_2Zr(N_2Ph_2)(py)$ (1.434(4) Å) and is more reminiscent of the late transition metal complexes $Ni(CNCMe_3)(N_2Ph)$ (1.385(5) Å) [38] and $Ni(P(p-tol)_3(N_2Ph_2)$ (1.371(6) Å) [39] in which the bonding of the N_2Ph_2 unit is more closely related to that of a π-bound azobenzene than a dianion. The N–N bond length in $Cp_2Ti(N_2Ph_2)$ is also significantly different than that of the titanium hydrazido(2$^-$) complex $(Ar'O)_2$-$(py)Ti(N_2Ph_2)$ $(Ar' = 2,6^iPrC_6H_3)$ recently reported by Durfree et al. [40]. Here the N–N bond distance of 1.416(8) Å is more reminiscent of that found in

---

* Reference number with asterisk indicates a note in the list of references.

Table 10

^{1}H NMR data

Compound	δ (ppm)	Mult	J (Hz)	Area	Assignment
1 ^{a}	0.04	s	–	3	CH_3
	3.89	s	–	1	N-H
	5.46	s	–	5	C_5H_5
	5.60	s	–	5	C_5H_5
	6.55	d	7.62	2	aromatic C-H
	6.72	d	7.48	2	aromatic C-H
	6.83	m	–	2	aromatic C-H
	7.01	t	8.23	2	aromatic C-H
	7.24	t	7.44	2	aromatic C-H
3 ^{b}	5.73	s	–	5	C_5H_5
	5.76	s	–	5	C_5H_5
	5.93	m	–	1	aromatic C-H
	6.02	m	–	1	aromatic C-H
	6.12	m	–	2	aromatic C-H
	6.75	m	–	4	aromatic C-H
	6.96	td	8.35, 1.50	1	aromatic C-H
	7.46	d	7.88	1	aromatic C-H
4 ^{c}	5.66	s	–	5	C_5H_5
	5.99	s	–	5	C_5H_5
	6.20	d	8.12	2	aromatic C-H
	6.34	m	–	2	aromatic C-H
	6.53	t	7.13	1	aromatic C-H
	6.90	m	–	3	aromatic C-H
	7.06	t	6.61	1	aromatic C-H
	7.23	td	7.56, 1.38	1	aromatic C-H
	7.61	t	6.65	2	aromatic C-H
	8.02	t	7.61	1	aromatic C-H
	9.13	d	5.03	2	aromatic C-H
5 ^{c}	1.48	d	6.76	9	CH_3
	5.68	d	1.71	5	C_5H_5
	5.72	d	1.85	5	C_5H_5
	6.03	m	–	1	aromatic C-H
	6.38	m	–	2	aromatic C-H
	6.53	d	7.66	2	aromatic C-H
	6.82	m	–	2	aromatic C-H
	6.91	t	7.28	2	aromatic C-H
	7.10	dt	1.61, 7.22	1	aromatic C-H
6 ^{d}	5.84	s	–	5	C_5H_5
	5.89	s	–	5	C_5H_5
	5.95	d	8.37	1	aromatic C-H
	6.39	m	–	3	aromatic C-H
	6.90	m	–	5	aromatic C-H
	7.09	d	6.90	1	aromatic C-H
	7.63	t	7.71	2	aromatic C-H
	7.80	t	7.65	1	aromatic C-H
	7.88	d	7.83	2	aromatic C-H
7 ^{a}	0.88	s	–	9	$C(CH_3)_3$
	5.69	s	–	5	C_5H_5
	5.66	s	–	5	C_5H_5
	6.79	m	–	2	aromatic C-H
	6.89	m	–	1	aromatic C-H
	7.20	m	–	6	aromatic C-H
	7.49	dt	1.41, 7.57	1	aromatic C-H

Table 10 (continued)

Compound	δ (ppm)	Mult	J (Hz)	Area	Assignment
8 [d]	1.81	d	–	3	CH_3
	1.88	s	–	3	CH_3
	5.83	s	–	5	C_5H_5
	5.98	s	–	5	C_5H_5
	6.31	dd	0.96, 7.23	1	aromatic C-H
	6.59	m	–	4	aromatic C-H
	6.70	t	7.26	1	aromatic C-H
	6.95	t	8.02	1	aromatic C-H
	7.09	t	7.99	2	aromatic C-H
	7.18	t	6.85	1	aromatic C-H
9 [d]	0.88	t	7.37	3	CH_3
	0.92	t	6.62	3	CH_3
	1.88	dq	14.16, 7.24	1	CH_2
	2.25	m	–	1	CH_2
	2.47	m	–	2	CH_2
	5.80	s	–	5	C_5H_5
	6.03	s	–	5	C_5H_5
	6.20	d	8.24	1	aromatic C-H
	6.60	m	–	4	aromatic C-H
	6.74	t	7.28	1	aromatic C-H
	6.96	t	7.77	1	aromatic C-H
	7.14	t	7.79	2	aromatic C-H
	7.20	t	7.88	1	aromatic C-H
10 [b]	5.99	s	–	5	C_5H_5
	6.06	s	–	5	C_5H_5
	6.66	m	–	3	aromatic C-H
	7.15	m	–	12	aromatic C-H
11 [a]	4.05	s	–	1	CH
	4.65	s	–	1	CH
	4.78	s	–	1	N-H
	5.87	s	–	5	C_5H_5
	6.00	s	–	5	C_5H_5
	6.66	d	6.76	2	aromatic C-H
	6.79	t	7.28	1	aromatic C-H
	6.87	m	–	3	aromatic C-H
	7.03	t	8.1	2	aromatic C-H
	7.18	m	–	5	aromatic C-H
	7.41	m	–	2	aromatic C-H

[a] C_6D_6, 22 °C. [b] THF-d_8, −20 °C. [c] CD_2Cl_2, 0 °C. [d] CD_2Cl_2, −40 °C.

$Cp_2Zr(N_2Ph_2)(py)$. In the dimer $\{[(^iPr_2PCH_2SiMe_2)_2N]ZrCl_2\}(N_2)$ the N–N bond distance was found to be 1.548(7) Å [41]. These bonds, however, are considerably longer than the N–N bond in *trans*-azobenzene (1.253(3) Å) [42].

Insight into the nature of the bonding and the hybridization of the nitrogens in the PhNNPh moiety can be gained by examination of the C_{ipso}–N–N–C_{ipso} torsional angle of the hydrazido ligand. In the crystal structures of the titanium and zirconium hydrazido(2^-) complexes the C_{ipso}–N–N–C_{ipso} torsional angles are 72 and 90°, respectively, indicating that there is no π bond between the two nitrogens of the hydrazido ligand whereas the analogous nickel complex exhibit

Table 11

$^{13}C\{^1H\}$ NMR data

Compound	δ (ppm)	Assignment	Compound	δ (ppm)	Assignment
1 [a]	20.06	CH_3	**7** [g,c]	30.07	$C(CH_3)_3$
	108.04	C_5H_5		59.36	$C(CH_3)_3$
	109.54	C_5H_5		109.14	C_5H_5
	113.30	aromatic C-H		109.32	C_5H_5
	117.47	aromatic C-H		112.29	aromatic C-H
	123.85	aromatic C-H		112.90	aromatic C-H
	128.29	aromatic C-H		114.44	aromatic C-H
	129.02	aromatic C-H		115.41	aromatic C-H
	129.63	aromatic C-H		116.92	aromatic C-H
	146.52	quat		117.23	aromatic C-H
	155.77	quat		128.09	aromatic C-H
				128.50	aromatic C-H
3 [b,c]	111.19	C_5H_5		129.38	aromatic C-H
	111.43	C_5H_5		129.53	aromatic C-H
	111.78	aromatic C-H		161.06	quat
	112.12	aromatic C-H		161.91	quat
	112.68	aromatic C-H	**8** [h,i]	17.73	CH_3
	113.21	aromatic C-H		20.99	CH_3
	117.38	aromatic C-H		108.75	C_5H_5
	119.80	aromatic C-H		109.99	C_5H_5
	126.60	aromatic C-H		111.98	aromatic C-H
	127.54	aromatic C-H		114.63	aromatic C-H
	127.98	aromatic C-H		116.10	aromatic C-H
	128.72	aromatic C-H		117.80	aromatic C-H
	161.15	quat		121.23	aromatic C-H
	163.22	quat		128.20	aromatic C-H
4 [d]	111.22	C_5H_5		128.29	aromatic C-H
	111.99	C_5H_5		128.69	aromatic C-H
	112.24	aromatic C-H		144.10	quat
	114.83	aromatic C-H		147.21	quat
	115.01	aromatic C-H		154.57	quat
	117.22	aromatic C-H		172.34	quat
	125.30	aromatic C-H	**9** [g,i]	13.87	CH_3
	128.08	aromatic C-H		16.43	CH_3
	128.50	aromatic C-H		24.94	CH_2
	128.79	aromatic C-H		28.68	CH_2
	139.58	aromatic C-H		108.57	C_5H_5
	152.93	aromatic C-H		109.83	C_5H_5
	160.06	quat		112.49	aromatic C-H
	162.54	quat		114.65	aromatic C-H
5 [e,c]	15.33 [l]	CH_3		116.62	aromatic C-H
	108.70	C_5H_5		117.42	aromatic C-H
	108.92	C_5H_5		118.87	aromatic C-H
	112.27	aromatic C-H		128.18	aromatic C-H
	113.52	aromatic C-H		128.39	aromatic C-H
	115.97	aromatic C-H		128.79	aromatic C-H
	116.48	aromatic C-H		144.87	quat
	118.89	aromatic C-H		151.93	quat
	128.06	aromatic C-H		153.79	quat
	128.50	aromatic C-H		183.37	quat
	128.63	aromatic C-H			

Table 11 (continued)

Compound	δ (ppm)	Assignment	Compound	δ (ppm)	Assignment
5 [e,c]	129.22	aromatic C-H	10 [g,i]	108.36	C_5H_5
	129.50	aromatic C-H		109.80	C_5H_5
	159.25	quat		117.16	aromatic C-H
	162.00	quat		117.24	aromatic C-H
				118.98	aromatic C-H
				123.85	C-C-Ph
6 [f,c]	110.65	C_5H_5		125.82	aromatic C-H
	110.70	C_5H_5		126.47	aromatic C-H
	111.68	aromatic C-H		128.02	aromatic C-H
	112.06	aromatic C-H		128.70	aromatic C-H
	114.04	aromatic C-H		129.24	aromatic C-H
	115.12	aromatic C-H		130.46	aromatic C-H
	116.26	aromatic C-H		143.25	quat
	116.48	aromatic C-H		146.30	quat
	127.60	aromatic C-H		154.74	quat
	127.94	aromatic C-H			
	128.86	aromatic C-H	11 [k]	85.21	CH_2
	129.08	aromatic C-H		112.62	C_5H_5
	129.83	aromatic C-H		112.51	C_5H_5
	131.20	quat		114.63	aromatic C-H
	132.16	quat		117.64	aromatic C-H
	132.76	aromatic C-H		118.43	aromatic C-H
	135.45	aromatic C-H		123.79	aromatic C-H
	160.67	quat		126.09	aromatic C-H
	160.88	quat		127.39	aromatic C-H
				128.22	aromatic C-H
				129.34	aromatic C-H
				129.78	aromatic C-H
				145.51	quat
				148.92	quat
				156.11	quat
				167.18	quat

[a] C_6D_6, 25°C. [b] THF-d_8 −20°C, complex 3 was only soluble enough in THF at this temperature to obtain spectra and therefore resonances for bound THF were not observed. [c] At this temperature neither of the phenyl rings of the hydrazido ligand are rotating freely on the NMR time scale. [d] CD_2Cl_2, −20°C. [e] CD_2Cl_2, −65°C. [f] CD_2Cl_2, −75°C. The resonance for the isonitrile carbon was not located. [g] CD_2Cl_2, −40°C. [h] CD_2Cl_2, −70°C. [i] Only one phenyl ring is freely rotating on the NMR time scale at this temperature. [j] The resonance for the α-carbon of the acetylide could not be found. [k] THF-d_8, 25°C. [l] This resonance is a doublet (J 18.6 Hz).

C_{ipso}–N–N–C_{ipso} torsional angles between 153 and 156°. The C_{ipso}–N–N–C_{ipso} torsional angle in cis-azobenzene is 8° [42].

In contrast to the insertion of internal alkynes into the Zr–N bond of 2, the reaction of 3 with phenylacetylene did not lead to a diazametallacycle but instead provided the acetylide $Cp_2Zr(NPhNHPh)(CCPh)$ (10) via a proton transfer from the alkyne to the η^2-hydrazido ligand as shown in eq. 8. An X-ray structure of 10 led to the ORTEP diagram shown in Fig. 3. Earlier precedents for this transformation include the reaction of the bisamide $Cp_2Zr(NMe_2)_2$ with terminal alkynes to provide $Cp_2Zr(CCR)_2$ and free amine [15a]. In a similar manner, addition of acetophenone to 3 also occurred by proton transfer, leading to the O-bound η^2-hydrazido(1⁻) enolate 11 (eq. 9). The mechanism of formation of 11 from 3

presumably involves displacement of THF by acetophenone, followed by proton transfer from the η^1-coordinated ketone to the η^2-hydrazido(2^-) ligand to give the observed product.

Experimental section

General: Unless otherwise noted, all manipulations were carried out under Ar or N_2 atmosphere in a Vacuum Atmospheres 553-2 drybox with attached M6-40-1H Dritrain, or by using standard Schlenk or vacuum-line techniques. Solutions were degassed as follows: they were cooled to $-196°C$, evacuated under high vacuum and thawed. This sequence was repeated three times in each case. Cylindrical glass reaction vessels fitted with ground glass joints and Teflon stopcocks are referred to as "bombs" throughout the experimental section.

^{1}H NMR spectra were obtained on either the 250, 300, 400 or 500 MHz Fourier Transform spectrometers at the University of California, Berkeley (UCB) NMR facility. The 250 and 300 MHz instruments were constructed by Mr. Rudi Nunlist and interfaced with either a Nicolet 1180 or 1280 computer. The 400 and 500 MHz instruments were commercial Bruker AM series spectrometers. ^{1}H NMR spectra were recorded relative to residual protiated solvent and are listed in Table 10. ^{13}C NMR spectra were obtained at either 75.4 or 100.6 MHz on the 300 or 400 MHz instruments, respectively, and chemical shifts were recorded relative to the solvent resonance. The ^{13}C{^{1}H} NMR data are listed in Table 11. Chemical shifts are reported in units of parts per million downfield from tetramethylsilane and all coupling constants are reported in Hz.

IR spectra were obtained on a Nicolet 510 FT-IR spectrometer. Mass spectroscopic (MS) analyses were obtained at the UCB mass spectrometry facility on AEI MS-12 and Kratos MS-50 mass spectrometers. Elemental analyses were obtained from the UCB Microanalytical Laboratory.

Sealed NMR tubes were prepared using Wilmad 505-PP and 504-PP tubes were attached via Cajon adapters directly to Kontes vacuum stopcocks and degassed using freeze-pump-thaw cycles before flame sealing [43]. Known volume bulb vacuum transfers were accomplished with an MKS Baratron gauge attached to a high vacuum line.

Unless otherwise specified, all reagents were purchased from commercial suppliers and used without further purification. Pentane and hexanes (UV grade, alkene free) were distilled from sodium benzophenone ketyl/tetraglyme under nitrogen. Benzene, toluene, ether and THF were distilled from sodium benzophenone ketyl under nitrogen. Deuterated solvents for use in NMR experiments were dried as their protiated analogues but were vacuum transferred from the drying agent. The preparation of $Cp_2Zr(Me)(Cl)$ was accomplished by literature methods [6]. Reagents used in this work were purified as follows: pyridine (Aldrich) was dried over Na and distilled under a nitrogen atmosphere, trimethylphosphine (Strem) was vacuum transferred from Na/K, benzonitrile and phenylacetylene (Aldrich) were stirred over P_2O_5 and distilled, t-butylisonitrile was dried over P_2O_5 and transferred to a bomb in which it was stored and vacuum transferred as needed, acetophenone (Aldrich) was dried over 3 Å sieves and distilled, 2-butyne and 3-hexyne (Aldrich) were stirred over Na and vacuum transferred, and 1,2-diphenylhydrazine, Cp_2ZrCl_2 and $[Cp_2Zr(H)Cl)]_n$ (Aldrich) were used without purification.

KNPhNHPh. Under an inert atmosphere, KH (210 mg, 5.25×10^{-4} mol), 1,2-diphenylhydrazine (1.252 g, 6.80×10^{-4} mol, 1.3 equiv) and 10 mL of toluene were combined in a Schlenk flask. The slurry was stirred for 6 d at $25\,^{\circ}$C and the reaction mixture was cooled to $-30\,^{\circ}$C, filtered, and washed with 5 mL of toluene. The solid was dried under vacuum to yield 865 mg (3.90×10^{-3} mol, 74%).

$Cp_2Zr(NPhNHPh)(Me)$ (1). To a solution of $Cp_2Zr(Me)(Cl)$ (243 mg, 8.94×10^{-4} mol) in 10 mL of THF at room temperature was added dropwise a solution of KNPhNHPh (209 mg, 9.38×10^{-4} mol, 1.05 equiv) in 5 mL of THF over 5 min. The resulting mixture was stirred for 1 d and the solvent removed under reduced pressure. The remaining solid was extracted with 10 mL of toluene, the extract was filtered and the volume of the filtrate reduced to 4 mL under vacuum. The toluene solution was layered with 3 mL of hexanes and cooled to $-30\,^{\circ}$C. Pale clumps grew under these conditions and were recovered by decanting the solvent and washing with cold hexanes to yield 311 mg (7.72×10^{-4} mol, 83%) of **1**. IR (C_6H_6): 3219w, 2924, 2012, 1921, 1886, 1592(s), 1275, 1213, 1153, 1077, 989, 852, 803 cm^{-1}; Found: C, 65.78; H, 5.79; N, 6.66. Anal. $C_{23}H_{24}N_2Zr$ calc.: C, 65.82; H, 5.76; N, 6.67%.

$Cp_2Zr(N_2Ph_2)(THF)$ (3) from Cp_2ZrCl_2. 1,2-Diphenylhydrazine (294 mg, 1.60×10^{-3} mol) was dissolved in 5 mL of ether and 2.05 mL of 1.56 *M* ^{n}BuLi in hexanes (3.20×10^{-3} mol, 2.0 equiv) was added dropwise at room temperature. As the ^{n}BuLi was added the ether solution turned from yellow to green. Upon addition of the last few drops of ^{n}BuLi the reaction mixture turned yellow and a white precipitate formed. After the solution had been stirred for 2 h, 5 mL of THF was added to dissolve the precipitate. To the solution of the $Li_2N_2Ph_2$ was added dropwise Cp_2ZrCl_2 (468 mg, 1.60×10^{-3} mol, 1 equivalent) as a solution in 5 mL of THF. The resulting brown solution turned yellow within 2 min and was stirred for an additional 2 h after which the volatile materials were removed under reduced pressure. The remaining solid was extracted into 30 mL of toluene, filtered and the solvent removed *in vacuo* to yield **3** as an off-white solid. In this manner $Cp_2Zr(N_2Ph_2)(THF)$ was prepared (723 mg, 1.52×10^{-3} mol, 95%) in > 90% purity as judged by ^{1}H NMR. Owing to difficulties in recrystallizing this complex it was normally used without further purification. However, the compound was recrystallized from toluene at $-30\,^{\circ}$C for spectroscopic characterization and combustion analysis. IR (C_6H_6): 1249, 730, 454 cm^{-1}; Anal. Found: C, 65.59; H, 5.81; N, 5.66. $C_{26}H_{28}N_2OZr$ calc.: C, 65.64; H, 5.93; N, 5.89%.

3 from $Cp_2Zr(H)(Cl)$. A solution of the mono-lithium salt of 1,2-diphenylhydrazine was prepared by dissolving 1,2-diphenylhydrazine (87.9 mg, 4.77×10^{-4} mol) in 5 mL of THF followed by dropwise addition of a solution of ^{n}BuLi (0.31 mL of 1.56 *M*, 4.77×10^{-4} mol) in hexanes. The resulting green solution was added dropwise at $25\,^{\circ}$C to a slurry of the polymeric $Cp_2Zr(H)(Cl)$ (123.6 mg, 4.77×10^{-4} mol) in 10 mL of THF. The solution became homogeneous in under 5 min and was stirred for 1 h. The volatile materials were removed under vacuum, the remaining solid was extracted with 20 mL of toluene, and the extract was filtered to remove LiCl. Removal of the toluene under reduced pressure left crude **3** as an off white solid (154 mg, 3.24×10^{-4} mol, 68%). Using this method **3** was typically isolated in 60–80% crude yield.

Generation of 3 by thermolysis of $Cp_2Zr(NPhNHPh)(Me)$ in THF. An NMR tube was loaded with $Cp_2Zr(NPhNHPh)(Me)$ (11.4 mg, 2.72×10^{-5} mol), the

internal standard p-dimethoxybenzene (2.7 mg, 1.96×10^{-5} mol) and 0.7 mL of THF-d_8. The solution was degassed, the NMR tube flame sealed and two one pulse ^{1}H NMR spectra were obtained in which the cyclopentadienyl resonance was integrated against the methyl resonance of the internal standard. The solution was heated for 3 h at 85 °C and the yield of **3** was determined by integration of its ^{1}H NMR spectrum and comparison with the original ^{1}H NMR spectra. Using this methodology the yield was determined to be 80%.

$Cp_2Zr(N_2Ph_2)(Py)$ (4). To a stirred solution of $Cp_2Zr(N_2Ph_2)(THF)$ (160 mg, 3.36×10^{-4} mol) in 10 mL of toluene at room temperature was added pyridine (27.9 mg, 3.53×10^{-4} mol, 1.05 equiv.). Upon addition of the pyridine the reaction mixture turned bright orange. The solution was stirred for 15 min and the volume of toluene was reduced to 3 mL under vacuum. Upon standing for several days at room temperature orange crystals formed and were isolated by decanting the solvent to yield 117 mg (2.43×10^{-4} mol, 72%) of **4**. IR (CH_2Cl_2) 1582, 1474, 1270, 1219, 758, 753, 697 cm^{-1}. We were unable to obtain satisfactory elemental analysis for this compound despite several recrystallizations of the sample.

$Cp_2Zr(N_2Ph_2)(PMe_3)$ (5). A bomb was charged with $Cp_2Zr(N_2Ph_2)(THF)$ (210 mg, 4.42×10^{-4} mol) and 15 mL of toluene and the solution degassed and cooled to -196 °C. PMe_3 (1.12×10^{-3} mol, 2.5 equiv) was transferred into the reaction vessel as a gas from a known volume bulb. The reaction mixture was warmed to room temperature and the resulting brown solution was stirred for 1 h and allowed to stand at room temperature. Brown crystals formed upon standing which were isolated by decanting the solvent to yield 176 mg (3.67×10^{-4} mol, 83%) of **5**. IR (CH_2Cl_2) 1583, 1478, 1308, 1276, 1237, 1157, 956, 804 cm^{-1}; Anal. Found: C, 62.24; H, 6.21; N, 5.62. $C_{25}H_{29}N_2PZr$ calc.: C, 62.59; H, 6.09; N, 5.84%. ^{31}P{^{1}H} NMR (CD_2Cl_2) δ -16.2 ppm.

$Cp_2Zr(N_2Ph_2)(NCPh)$ (6). To a stirred solution of $Cp_2Zr(N_2Ph_2)(THF)$ (286 mg, 6.01×10^{-4} mol) in 5 mL of toluene at room temperature was added dropwise benzonitrile (75 mg, 7.21×10^{-4} mol, 1.2 equiv). The color of the solution changed from pale yellow to brown upon addition of the benzonitrile. The reaction mixture was stirred for 30 min and the volatile materials were removed under reduced pressure to leave a red-brown oil. The oil was dissolved in 4 mL of ether and cooled to -30 °C. Under these conditions crystals formed and were isolated by decanting the solvent and washing with cold toluene to yield 205 mg (4.15×10^{-4} mol, 69%) of **6**. IR (Nujol): 2256w, 1579, 1301, 1289, 1252, 799, 746, 493, 473 cm^{-1}; Anal. Found: C, 67.92; H, 5.04; N, 9.03. $C_{28}H_{25}N_3Zr$ calc.: C, 67.98; H, 5.09; N, 8.49%.

$Cp_2Zr(N_2Ph_2)(CNCMe_3)$ (7). A bomb was charged with $Cp_2Zr(N_2Ph_2)(THF)$ (1.88 mg, 3.95×10^{-4} mol) and 15 mL of toluene and the solution was degassed and cooled to -196 °C. t-Butylisocyanide (7.90×10^{-4} mol, 2.0 equiv) was added by vacuum transfer from a known volume bulb. The solution was thawed and the resulting orange reaction mixture was stirred for 20 min at room temperature after which the volatile materials were removed under reduced pressure. The remaining solid was dissolved in 5 mL of ether and filtered to remove a small amount of insoluble material. The ether solution was chilled to -30 °C at which temperature yellow flakes formed. This mixture was poured onto a filter frit which had been pre-cooled to -30 °C and suction filtered to yield 150 mg (3.08×10^{-4} mol, 78%) of **7**. IR (CH_2Cl_2): 2200w, 1299, 750, 741, 670, 455 cm^{-1}; Anal. Found: C, 67.03; H, 6.34; N, 8.43. $C_{26}H_{28}N_2Zr$ calc.: C, 66.62; H, 6.01; N, 8.63%.

Cp₂Zr[PhNN(Ph)C(Me)C(Me)] (8). A bomb was loaded with $Cp_2Zr(N_2Ph_2)$-(THF) (411 mg, 8.64×10^{-4} mol), 15 mL of toluene and a stir bar. The solution was degassed and cooled to $-196\,°C$. 2-Butyne (3.46×10^{-3} mol, 4 equiv) was added to the bomb by vacuum transfer from a known volume bulb. The solution was thawed and heated with stirring for 24 h at $65\,°C$ during which time the color changed to dark brown. The volume of toluene was reduced to 4 mL under reduced pressure and 2 mL of hexanes was added. After standing at room temperature for several days orange-brown crystals grew and were isolated by decanting the solvent to provide 308 mg (6.74×10^{-4} mol, 78%) of **8**. IR (C_6H_6): 1588, 1573, 1494, 1296, 1268, 1253, 803, 760, 751, 481, 470, 456, 450, 443 cm^{-1}. Elemental analysis was not attempted on this compound in light of the successful determination of its structure by X-ray diffraction and the satisfactory analysis of the closely related **9**.

Cp₂Zr[PhNN(Ph)C(Et)C(Et)] (9). A glass bomb was charged with Cp_2Zr $(N_2Ph_2)(THF)$ (270 mg, 5.68×10^{-4} mol), 3-hexyne (233 mg, 2.48×10^{-3} mol, 5 equiv), 10 mL of toluene and a stir bar. The solution was degassed and heated to $45\,°C$ for 5 d with stirring. The volatile materials were removed from the resulting brown solution under reduced pressure. The remaining brown solid was dissolved in ether and chilled to $-30\,°C$ to give orange-brown crystals containing 1/2 equivalent of ether (quantified by ^1H NMR integration). The crystals were isolated by decanting the solvent and washing with hexanes to yield 270 mg (5.17×10^{-4} mol, 91%) of **9 · 1/2Et₂O**. IR (CH_2Cl_2) 1589, 1485, 1479, 1447, 1439, 1298, 1168, 1021, 1015, 895, 881, 807 cm^{-1}; Anal. Found: C, 68.93; H, 6.85; N, 5.26. $C_{28}H_{30}N_2Zr \cdot 1/2Et_2O$ calc.: C, 68.93; H, 6.75; N, 5.36%.

Complex 9 from Cp₂Zr(NPhNHPh)(Me). An NMR tube was loaded with $Cp_2Zr(NPhNHPh)(Me)$ (9.3 mg, 2.22×10^{-5} mol), 3-hexyne (7.5 mg, 9.13×10^{-5} mol, 4.1 equiv), *p*-dimethoxybenzene (3.5 mg, 2.54×10^{-5} mol) as an internal ^1H NMR standard and 0.7 mL of C_6D_6. The solution was degassed and the NMR tube flame sealed. An initial ^1H NMR spectrum was acquired in which the resonance for the cyclopentadienyl ligands was integrated against the methyl resonance of the internal standard. After 3 h at $85\,°C$ ^1H NMR spectrometry indicated all **1** had been consumed and metallacycle **9** and methane had been produced. Integration of the ^1H NMR spectrum as described above and comparison with the initial ^1H NMR spectrum indicated the product had been formed in 89% yield.

Cp₂Zr(NPhNHPh)(CCPh) (10). To a stirred solution of $Cp_2Zr(N_2Ph_2)(THF)$ (342 mg, 7.18×10^{-4}) in 15 mL of toluene at room temperature was added dropwise phenylacetylene (164 mg, 1.61×10^{-3} mol, 2.2 equiv). The solution was stirred for 1 h, filtered to remove a fine precipitate, and the volume of filtrate was reduced to 4 mL under vacuum. The solution was layered with 2 mL of pentane and cooled to $-30\,°C$. Pale yellow crystals which formed under these conditions were isolated by filtration to yield 254 mg (4.62×10^{-3} mol, 64%) of crystals containing 1/2 equivalent of toluene per molecule **10** (quantified by ^1H NMR integration and X-ray crystallography). IR (Nujol) 3205, 1591, 1507, 1488, 1482, 1467, 1440, 1377, 1310, 1272, 1200, 1017, 1011, 857, 827, 811, 801, 785, 761, 757, 748, 735, 692, 615, 591, 537, 508 cm^{-1}; MS (FAB, 4-nitrophenyl (n-octyl)ether matrix): m/e 506 (M^+). Anal. Found: C, 73.27; H, 5.61; N, 4.94. $C_{30}H_{26}N_2Zr \cdot 1/2C_7H_8$ calc.: C, 72.91; H, 5.48; N, 5.08%.

Cp₂Zr(NPhNHPh)(OC(=CH₂)Ph) (11). To a stirred solution of Cp_2Zr $(N_2Ph_2)(THF)$ (3.78×10^{-4} mol) in 10 mL of benzene at room temperature was added dropwise acetophenone (49 mg, 4.08×10^{-4} mol, 1.1 equiv). The pale yellow solution was stirred for 5 min and the volatile materials were removed under reduced pressure. The remaining solid was dissolved in 4 mL of toluene and hexanes was diffused in the solution at $-30\,°C$ by vapor phase diffusion over several days. White clusters of **11** formed under these conditions to provide 138 mg (2.53×10^{-4} mol, 67%). IR (CH_2Cl_2): 3240w, 1591, 1484, 1442, 1316, 1303, 1288, 809, 583, 559, 464 cm^{-1}; MS (FAB, tetraglyme) 524(MH^+). We were unable to obtain satisfactory combustion analysis on this compound.

Structural data for 4: general technique for structure determination

Isolation and mounting

Pale yellow prismatic crystals of the compound were obtained by slow crystallization from a 50/50 mixture of toluene and hexane. Fragments cleaved from some of these crystals were mounted in thin-wall glass capillaries in an inert-atmosphere glove box and then flame sealed. Preliminary precession photographs indicated orthorhombic Laue symmetry and yielded approximate cell dimensions.

The crystal used for data collection was then transferred to our Enraf-Nonius CAD-4 diffractometer and centered in the beam. Automatic peak search and indexing procedures yielded the orthorhombic reduced primitive cell. The final cell parameters and specific data collection parameters for this data set are given in Table 1.

Structure determination

The 3372 raw intensity data were converted to structure factor amplitudes and their esd's by correction for scan speed, background, and Lorentz and polarization effects. No correction for crystal decomposition was necessary. Inspection of the azimuthal scan data showed a variation $I_{min}/I_{max} = \pm 2\%$ for the average curve. No correction for absorbtion was applied. Inspection of the systematic absences indicated uniquely space group *Pbca*. Removal of systematically absent data left 2978 unique data in the final data set.

The structure was solved by Patterson methods and refined via standard least-squares and Fourier techniques [44]. In a difference Fourier map calculated following the refinement of all non-hydrogen atoms with anisotropic thermal parameters, peaks were found corresponding to the positions of all the hydrogen atoms. Hydrogen atoms were assigned idealized locations and values of B_{iso} approximately 1.2 times the B_{eq} of the atoms to which they were attached. They were included in the structure factor calculations, but not refined.

The final residuals for 280 variables refined against the 1643 data for which $F^2 > 3\sigma(F^2)$ were $R = 2.78\%$, $wR = 3.04\%$ and $GOF = 1.246$. The R value for all 2978 data was 19.1%. The reason for the substantial difference between R(data used) and R(all) is that the full 2978 unique data points contained a large number of net intensity values that were measured as negative, rather than zero or slightly positive, due to random scatter or background problems. In these cases the structure factor amplitudes are assigned (meaningless) negative values, and the program flags the values let the user know about the problem. When this situation

Table 12

Positional parameters for complex **4**

Atom	x	y	z	B (Å^2)
Zr	0.16803(3)	0.14014(3)	0.08931(2)	3.108(7)
N1	0.0538(2)	0.1502(2)	0.1602(2)	3.69(8)
N2	0.0382(2)	0.1986(2)	0.0999(2)	3.79(9)
N3	0.1455(2)	0.1863(2)	−0.0275(2)	3.79(9)
C1	0.1852(5)	−0.0080(3)	0.1255(3)	6.1(1)
C2	0.1080(4)	−0.0072(3)	0.0841(3)	5.2(1)
C3	0.1365(4)	0.0094(3)	0.0194(2)	5.2(1)
C4	0.2321(4)	0.0181(3)	0.0204(3)	6.2(1)
C5	0.2610(4)	0.0042(3)	0.0857(3)	6.8(1)
C6	0.2594(4)	0.2750(3)	0.0885(3)	5.2(1)
C7	0.3238(3)	0.2114(3)	0.0830(2)	4.9(1)
C8	0.3230(4)	0.1688(3)	0.1449(2)	5.6(1)
C9	0.2586(4)	0.2041(3)	0.1861(2)	5.9(1)
C10	0.2194(4)	0.2705(3)	0.1524(3)	5.8(1)
C11	−0.0185(3)	0.0965(3)	0.1771(2)	3.8(1)
C12	−0.1041(4)	0.0963(3)	0.1439(2)	4.7(1)
C13	−0.1736(4)	0.0419(4)	0.1635(3)	6.0(1)
C14	−0.1598(4)	−0.0124(3)	0.2171(3)	6.4(1)
C15	−0.0763(4)	−0.0121(3)	0.2508(3)	5.7(1)
C16	−0.0076(4)	0.0426(3)	0.2322(2)	4.7(1)
C17	−0.0024(3)	0.2743(3)	0.1093(2)	4.0(1)
C18	−0.0527(3)	0.2939(3)	0.1687(3)	5.0(1)
C19	−0.0967(4)	0.3708(4)	0.1743(3)	6.9(2)
C20	−0.0924(4)	0.4286(4)	0.1233(3)	7.7(2)
C21	−0.0418(4)	0.4111(4)	0.0654(3)	6.9(2)
C22	0.0029(4)	0.3347(3)	0.0584(3)	5.3(1)
C23	0.0596(3)	0.1813(3)	−0.0533(3)	4.4(1)
C24	0.0379(3)	0.2037(4)	−0.1193(2)	4.9(1)
C25	0.1067(4)	0.2344(4)	−0.1608(3)	6.2(2)
C26	0.1942(4)	0.2386(4)	−0.1349(3)	6.9(2)
C27	0.2115(3)	0.2130(4)	−0.0688(2)	5.0(1)

occurs the negative structure factor amplitudes are all "unobserved", of course, and contribute heavily to R(all). We checked carefully, and there were no very large values of F_{calc} for the unobserved data.

The quantity minimized by the least-squares program was $\Sigma w(|F_o| - |F_c|)^2$, where w is the weight of a given observation. The p-factor, used to reduce the weight of intense reflections, was set to 0.03 throughout the refinement. The analytical forms of the scattering factor tables for the neutral atoms were used and all scattering factors were corrected for both the real and imaginary components of anomalous dispersion.

Inspection of the residuals ordered in ranges of $\sin(\theta/\lambda)$, $|F_o|$, and parity and value of the individual indexes showed no unusual features or trends. The largest peak in the final difference Fourier map had an electron density of 0.20 e$^-$/Å^3, and the lowest excursion −0.17 e$^-$/Å^3. There was no indication of secondary extinction in the high-intensity low-angle data.

The positional parameters of the non-hydrogen atoms for the structure of **4** (as well as for **8** and **10**; see below) are given in Tables 12–14.

Table 13

Positional parameters for complex **8** [a]

Atom	x	y	z	B (Å²)
Zr1	−0.06373(2)	−0.16938(5)	0.000	1.714(8)
N1	0.0539(2)	−0.1315(5)	−0.0024(2)	2.18(8)
N2	0.0549(2)	−0.1250(6)	−0.0515(1)	2.41(9)
C1	0.0093(3)	−0.0040(6)	−0.0739(2)	2.0(1)
C2	−0.0604(3)	0.0123(6)	−0.0577(2)	2.1(1)
C3	0.0481(3)	0.0927(7)	−0.1113(2)	3.0(1)
C4	−0.1132(3)	0.1423(7)	−0.0771(2)	3.0(1)
C11	0.113793	−0.0502(6)	0.0190(2)	2.0(1)
C12	0.1533(3)	0.0754(6)	−0.0012(2)	2.4(1)
C13	0.2098(3)	0.1557(7)	0.0228(2)	3.1(1)
C14	0.2278(3)	0.1129(7)	0.0666(2)	3.2(1)
C15	0.1897(3)	−0.0124(8)	0.0869(2)	3.1(1)
C16	0.1340(3)	−0.0948(7)	0.0632(2)	2.5(1)
C21	0.0977(3)	−0.2451(7)	−0.0740(2)	2.1(1)
C22	0.1465(3)	−0.3432(7)	−0.0492(2)	2.5(1)
C23	0.1866(3)	−0.4663(7)	−0.0711(2)	3.2(1)
C24	0.1765(3)	−0.4945(7)	−0.1177(2)	3.2(1)
C25	0.1279(3)	−0.3974(8)	−0.1418(2)	3.1(1)
C26	0.0883(3)	−0.2737(7)	−0.1210(2)	2.7(1)
C51	−0.0484(3)	0.0313(7)	0.0653(2)	2.6(1)
C52	−0.1109(3)	0.0800(7)	0.0398(2)	2.6(1)
C53	−0.1679(3)	−0.0363(7)	0.0440(2)	2.6(1)
C54	−0.1403(3)	−0.1595(7)	0.0728(2)	2.6(1)
C55	−0.0652(3)	−0.1181(7)	0.0850(2)	2.7(1)
C56	−0.1102(3)	−0.4561(6)	0.0070(2)	2.9(1)
C57	−0.1693(3)	−0.3735(6)	−0.0136(2)	2.7(1)
C58	−0.1464(3)	−0.3219(7)	−0.0568(2)	2.7(1)
C59	−0.0720(3)	−0.3775(7)	−0.0637(2)	3.4(1)
C60	−0.0479(3)	−0.4606(7)	−0.0245(2)	2.9(1)
Zr2	−0.27512(2)	−0.55331(5)	−0.27337(2)	1.493(7)
N3	−0.1672(2)	−0.6058(5)	−0.3012(1)	1.74(8)
N4	−0.1354(2)	−0.6709(5)	−0.2602(1)	2.05(8)
C5	−0.1399(3)	−0.5773(6)	−0.2180(2)	1.7(1)
C6	−0.2063(3)	−0.5034(6)	−0.2103(2)	2.2(1)
C7	−0.0679(3)	−0.5607(6)	−0.1905(2)	2.6(1)
C8	−0.2177(3)	−0.4025(7)	−0.1674(2)	3.2(1)
C31	−0.1135(3)	−0.5503(6)	−0.3329(2)	1.9(1)
C32	−0.0367(3)	−0.5283(6)	−0.3229(2)	2.5(1)
C33	0.0111(4)	−0.4639(7)	−0.3556(3)	4.8(2)
C34	−0.0158(4)	−0.4217(7)	−0.3981(3)	5.7(1)
C35	−0.0910(4)	−0.4449(8)	−0.4088(2)	5.7(2)
C36	−0.1398(3)	−0.5105(7)	−0.3771(2)	3.2(1)
C41	−0.1122(2)	−0.8325(5)	−0.2597(2)	1.8(1)
C42	−0.0981(3)	−0.9152(6)	−0.3007(2)	1.9(1)
C43	−0.0763(3)	−1.0744(6)	−0.2995(2)	2.4(1)
C44	−0.0664(3)	−1.1555(6)	−0.2583(2)	2.5(1)
C45	−0.0809(3)	−1.0753(6)	−0.2178(2)	2.4(1)
C46	−0.1037(3)	−0.9157(6)	−0.2182(2)	2.1(1)
C61	−0.3758(3)	−0.7524(8)	−0.2932(2)	3.5(1)
C62	−0.3118(3)	−0.8448(6)	−0.2853(2)	2.9(1)
C63	−0.2939(3)	−0.8321(6)	−0.2387(2)	2.4(1)
C64	−0.3496(3)	−0.7324(6)	−0.2190(2)	2.6(1)

Table 13 (continued)

Atom	x	y	z	B (Å^2)
C65	−0.3996(3)	−0.6862(7)	−0.2524(2)	3.1(1)
C66	−0.3738(3)	−0.3649(6)	−0.3046(2)	2.4(1)
C67	−0.3131(3)	−0.3599(6)	−0.3352(2)	2.2(1)
C68	−0.2507(3)	−0.2858(6)	−0.3130(2)	2.5(1)
C69	−0.2736(3)	−0.2491(6)	−0.2680(2)	2.9(1)
C70	−0.3500(3)	−0.2994(6)	−0.2634(2)	2.9(1)

[a] The thermal parameter given for anisotropically refined atoms is the isotropic equivalent thermal parameter defined as: $(4/3)[a^2\beta(1,1) + b^2\beta(2,2) + c^2\beta(3,3) + ab(\cos \gamma)\beta(1,2) + ac(\cos \beta)\beta(1,3) + bc(\cos \alpha)\beta(2,3)]$; where a, b, c are real cell parameters, and $\beta(i,j)$ are anisotropic betas.

Table 14

Positional parameters for complex **10**

Atom	x	y	z	B (Å^2)
Zr	0.19930(8)	0.24231(2)	0.30092(4)	1.50(1)
N1	−0.0028(6)	0.2249(2)	0.4005(3)	1.5(1)
N2	0.1134(6)	0.2725(2)	0.4203(3)	1.7(1)
C1	−0.038(8)	0.1766(3)	0.4623(4)	1.7(1)
C2	−0.1178(8)	0.1300(3)	0.4393(4)	1.7(1)
C3	−0.1214(9)	0.0825(3)	0.4963(5)	2.6(2)
C4	−0.0151(8)	0.0807(3)	0.5753(4)	2.4(1)
C5	0.0975(8)	0.1277(3)	0.5974(4)	2.3(1)
C6	0.1057(8)	0.1757(3)	0.5410(4)	1.8(1)
C7	0.0591(8)	0.3194(3)	0.4691(4)	1.8(1)
C8	−0.870(8)	0.3174(3)	0.5143(4)	2.0(1)
C9	−0.1275(8)	0.3662(3)	0.5640(4)	2.3(1)
C10	−0.0276(9)	0.4169(3)	0.5695(5)	3.0(2)
C11	0.1153(9)	0.4196(3)	0.5230(5)	3.1(2)
C12	0.1552(9)	0.3721(3)	0.4725(5)	2.7(2)
C13	0.1107(8)	0.1502(3)	0.2573(4)	1.9(1)
C14	0.0480(9)	0.1027(3)	0.2340(4)	2.4(1)
C15	−0.0286(9)	0.0461(3)	0.2044(4)	2.3(1)
C16	−0.1748(9)	0.0244(3)	0.2387(5)	2.9(2)
C17	−0.2529(9)	−0.0283(3)	0.2074(5)	3.0(2)
C18	−0.1871(9)	−0.0603(3)	0.1418(5)	2.7(2)
C19	−0.0434(9)	−0.0398(3)	0.1072(5)	3.1(2)
C20	0.0355(9)	0.0133(3)	0.1381(5)	3.0(2)
C21	0.4749(9)	0.1798(3)	0.3143(5)	3.2(2)
C22	0.4977(8)	0.2263(3)	0.2574(4)	3.1(2)
C23	0.5063(9)	0.2797(3)	0.3061(5)	2.9(2)
C24	0.4890(8)	0.2653(3)	0.3937(4)	2.6(1)
C25	0.4649(9)	0.2041(3)	0.3980(5)	2.8(2)
C26	−0.025(1)	0.3189(3)	0.2473(5)	4.3(2)
C27	−0.0710(8)	0.2677(4)	0.1980(5)	3.5(2)
C28	0.0586(9)	0.2580(3)	0.1430(4)	3.0(1)
C29	0.1826(9)	0.3021(3)	0.1593(5)	3.1(2)
C30	0.132(1)	0.3391(3)	0.2247(5)	4.1(2)
C31	0.387(1)	0.0476(3)	0.4731(7)	6.6(2)
C32	0.458(1)	0.0432(3)	0.5600(7)	6.0(2)
C33	0.572(1)	−0.0043(4)	0.5886(6)	5.7(2)
C34	0.635(2)	−0.0072(6)	0.666(1)	3.4(4)

Structural data for 8

Isolation and mounting

Clear, orange, wedge-shaped crystals of the compound grew on the side of the vessel upon crystallization by vapor diffusion of hexane into a toluene solution of **8** at room temperature. Fragments cleaved from some of these crystals were mounted in this-wall glass capillaries in an inert-atmosphere glove box and then flame sealed.

During data collection the crystal was cooled to $-108\,^\circ$C by a nitrogen flow low-temperature apparatus which had been previously calibrated by a thermocouple placed at the sample position. The final cell parameters and specific data collection parameters for this data set are given in Table 1.

Structure determination

The 3189 raw intensity data were reduced as above. No correction for the crystal decomposition or absorption was necessary. Inspection of the systematic absences indicated possible space group $Pna2_1$ or $Pnam$. The choice of the acentric group was confirmed by the successful solution and refinement of the structure. Removal of systematically absent data left 2837 unique data in the final data set.

The structure was solved using techniques outlined in the structural determination of **4** as outlined above. In the final cycles, one reflection (004) was removed from the data set due to possible effects of secondary extinction. A refinement test for correctness of the assigned enantiomorph of the crystal was performed.

The final residuals for 522 variables refined against the 2497 data for which $F^2 > 3\sigma(F^2)$ were $R = 2.18\%$, $wR = 2.55\%$, and $GOF = 1.183$. The R value for all 2837 data was 4.49%. The p-factor, was set to 0.03 throughout the refinement. The largest peak in the final difference Fourier map had an electron density of 0.20 $e^-/\mathring{A}^3$, and the lowest excursion -0.17 $e^-/\mathring{A}^3$. There was no indication of secondary extinction in the high-intensity low-angle data.

Structural data for 10

Isolation and mounting

The air-sensitive crystals of the compound were crystallized from toluene. The yellow crystals were placed in a high molecular weight oil (Paratone N, Exxon) in an inert atmosphere box. The crystal used for data collection was quickly cooled to $-100\,^\circ$C by a nitrogen flow low-temperature apparatus. Automatic peak search and indexing procedures yielded a monoclinic reduced primitive cell. Inspection of the Niggli values revealed no conventional cell of higher symmetry. The final cell parameters and specific data collection parameters for this data set are given in Table 1.

Structure determination

The raw intensity data were reduced as above. No correction for crystal decomposition was necessary. An empirical correction based on the observed variation was applied to the data. Inspection of the systematic absences uniquely indicated the space group $P2_1/n$. Removal of systematically absent and redundant data left 3446 data in the final data set.

The structure was solved using techniques described above for the structure determination of **4**. Hydrogen atoms were assigned idealized locations and values of $B_{iso} = 1.3$ times the B_{eq} of the atoms to which they were attached. Hydrogens were included in structure calculations, but not refined.

The final residuals for 334 parameters refined against the 2196 data for which $F^2 > 3\sigma$ were $R = 4.0\%$, $wR = 4.9\%$ and $GOF = 1.25$. The R value for all 3446 data was 10.8%. The p-factor was set to 0.05 in the last cycles of the refinement. The largest peak in the final difference Fourier maps had an electron density of 0.431 e$^-$/Å^3, and the lowest excursion 0.320 e$^-$/Å^3. There was no indication of secondary extinction in the high-intensity low-angle data. The analytical forms of the scattering factor tables for the neutral atoms were used and all scattering factors were corrected for both the real and imaginary components of anomalous dispersion.

Acknowledgments

References and notes

1 (a) M.F. Lappert, P.P. Power, A.R. Sanger and R.C. Srivastava, Metal and Metalloid Amides, Ellis Horwood Limited: West Sussex, England, 1980. For a comparison of the relative insertion reactivities of group 4 metal amide and alkyls complexes see: (b) R.A. Andersen, Inorg. Chem., 18 (1979) 2928.

2 D.C. Bradley, R.C. Mehrotra and D.P. Gaur, Metal Alkoxides, Academic Press, San Francisco, CA, 1978.

3 (a) H.E. Bryndza and W. Tam, Chem. Rev., 88 (1988) 1163; (b) M.D. Fryzuk and C.D. Montgomery, Coord. Chem. Rev., 95 (1989) 1; (c) M.R. Gagné and T.J. Marks, J. Am. Chem. Soc., 111 (1989) 4108; (d) A.L. Casalnuovo, J.C. Calabrese and D. Milstein, J. Am. Chem. Soc., 110 (1988) 6738; (e) R.L. Cowan and W.C. Trogler, Organometallics, 6 (1987) 2451.

4 (a) G. Erker, U. Dorf, P. Czisch and J.L. Petersen, Organometallics, 5 (1986) 668 and references therein: (b) S.L. Buchwald, M.W. Wannamaker and B.T. Watson, J. Am. Chem. Soc., 111 (1989) 776; (c) S.L. Buchwald, B.T. Watson, M.W. Wannamaker and J.C. Dewan, J. Am. Chem. Soc., 111 (1989) 4486; (d) E.J. Roskamp and S.F. Pedersen, J. Am. Chem. Soc., 109 (1987) 6551; (e) R.B. Nielsen and S.L. Buchwald, J. Am. Chem. Soc., 110 (1988) 3171; (f) R.B. Nielsen and S.L. Buchwald, J. Am. Chem. Soc., 109 (1987) 1590; (g) A portion of the work described in this paper has been published in preliminary form: P.J. Walsh, F.J. Hollander and R.G. Bergman, J. Am. Chem. Soc., 112 (1990) 894.

5 I.A. Latham, G.J. Leigh, G. Huttner and I. Jibril, J. Chem. Soc., Dalton Trans., (1986) 385.

6 (a) P.C. Wailes, H. Weigold and A.P. Bell, J. Organomet. Chem., 34 (1971) 155; (b) P.J. Walsh, F.J. Hollander and R.G. Bergman, J. Am. Chem. Soc., 110 (1988) 8729.

7 G. Wittig, Angew. Chem., 53 (1940) 241.

8 N–N single bond distances in compounds of the type R_2N–NH_2 are ~ 1.45 Å, see The Handbook of Chemistry and Physics, 50th ed., CRC Press, Cleveland, 1969, pp. F154–F157.

9 The Zr–N distance in the η^2-imine complex $Cp_2Zr(CHPhNSiMe_3)(THF)$ is 2.11(1), see ref. 4b. The Zr–N bond distance in $Cp_2^*Zr(=S)(4$-t-butylpyridine) is 2.341(4) Å, see M.J. Carney, P.J. Walsh, F.J. Hollander and R.G. Bergman, J. Am. Chem. Soc., 112 (1990) 6426.

10 For coordination of pyridine to Zr^{IV} see: P. Tomasik and Z. Ratajewicz, in G.R. Newkome and L. Strekowksi (Eds.), Pyridine–Metal Complexes, Intersciences, New York, 1985, pp. 708.

11 (a) G. Chandra, T.A. George, M.F. Lappert and R.C. Srivastava, J. Chem. Soc. A, (1970) 2550; for an example of insertion of a nitrile into the Sc–N bond of a hydrazido(1^-) complex see; (b) P.J. Shapiro, L.M. Henling, R.E. Marsh and J.E. Bercaw, Inorg. Chem., 29 (1990) 4560.

12 (a) B.N. Storhoff and H.C. Lewis Jr., Coord. Chem. Rev., 23 (1977) 1. Free benzonitrile in Nujol absorbs at 2231 cm^{-1}; (b) R.A. Walton, Q. Rev., Chem. Soc., 19 (1965) 126.

13 (a) D.L. Thorn and R. Hoffmann, Nouv. J. Chem., 3 (1979) 39; for examples of non-planar heterometallacycles see: (b) R.L. Chamberlain, L.D. Durfee, P.E. Fanwick, L.M. Kobriger, S.I. Latesky, A.K. McMullin, B.D. Steffey, I.P. Rothwell, K. Folting and J.C. Huffman, J. Am. Chem. Soc., 109 (1987) 6068; (c) M.D. Curtis and J. Real, J. Am. Chem. Soc., 108 (1986) 4668; P. Hofmann, M. Frede, P. Stauffert, W. Lasser and U. Thewalt, Angew. Chem., Int. Ed. Eng., 24 (1985) 712.

14 For example the ^{13}C resonance for the corresponding sp^2-hybridized carbon in Cp$_2^*$ZrPh$_2$ is 193.5 ppm; see: L.E. Schock, C.P. Brock and T.J. Marks, Organometallics, 6 (1987) 232. In the metallacycle Cp$_2$Zr(CPhCPhCHNSiMe$_3$) the sp^2-hybridized carbon resonates at 187.0 ppm; see ref. 4b.

15 (a) G. Chandra, M.F. Lappert and R.C. Srivastava, J. Chem. Soc. A, (1968) 1940; (b) A.D. Jenkins, M.F. Lappert and R.C. Srivastava, J. Chem. Soc., (1965) 2157; (c) M.R. Collier, M.F. Lappert and J. McMeeking, Inorg. Nucl. Chem. Lett., 7 (1971) 689.

16 G. Erker, W. Frömberg, R. Benn, R. Mynott, K. Angermund and C. Krüger, Organometallics, 8 (1989) 911.

17 (a) C.P. Gibson, G. Gaddagh and S.H. Bertz, J. Chem. Soc., Chem. Commun., (1988) 603; (b) M.D. Curtis, S. Thanedar and W.M. Butler, Organometallics, 3 (1984) 1855; (c) J.R. Stille and R.H. Grubbs, J. Am. Chem. Soc., 105 (1983) 1664.

18 The methylene carbon of the enolate Cp$_2^*$Zr(OCH=CH$_2$)(H) resonates at 89.4 ppm in the ^{13}C{^{1}H} NMR; see E.J. Moore, D.A. Straus, J. Armantrout, B.D. Santarsiero, R.H. Grubbs and J.E. Bercaw, J. Am. Chem. Soc., 105 (1983) 2069.

19 G. Erker, J. Organomet. Chem., 134 (1977) 189 and references therein.

20 S.L. Buchwald, B.T. Watson and J.C. Huffman, J. Am. Chem. Soc., 108 (1986) 7411.

21 (a) J.W. Lauher and R. Hoffmann, J. Am. Chem. Soc., 98 (1976) 1729; (b) J.C. Green, S.E. Jackson and B. Higginson, J. Chem. Soc., Dalton Trans., (1975) 403; (c) J.L. Petersen and L.F. Dahl, J. Am. Chem. Soc., 97 (1975) 6422; (d) J.L. Petersen and L.F. Dahl, J. Am. Chem. Soc., 97 (1975) 6416; (e) J.L. Petersen, D.L. Lichtenberger, R.F. Fenske and L.F. Dahl, J. Am. Chem. Soc., 97 (1975) 6433; (f) H.H. Brintzinger, L.L. Lohr and K.T.L. Wong, J. Am. Chem. Soc., 97 (1975) 5146; (g) J.H. Ammeter, N. Oswald and R. Bucher, Helv. Chim. Acta, 58 (1975) 671; (h) J.L. Petersen and L.F. Dahl, J. Am. Chem. Soc., 97 (1974) 2248; (i), J.C. Green, M.L.H. Green and C.K. Prout, J. Chem. Soc., Chem. Commun., (1972) 421; (j) M.L.H. Green, Pure Appl. Chem., 30 (1972) 373; (k) H.H. Brintzinger and L.S. Bartell, J. Am. Chem. Soc., 92 (1970) 1105; (l) M.W. Alcock, J. Chem. Soc. A, (1967) 2001; (m) C. Ballhausen and J.P. Dahl, Acta Chim. Scand., 15 (1961) 1333.

22 Examples of η^1-hydrazido(1^-) ligands see: (a) J.A. McCleverty, A.E. Rea, I. Wolochowicz, N.A. Bailey and J.M.A. Smith, J. Chem. Soc., Dalton Trans., (1983) 71; (b) C.F. Barrientos-Penna, C.F. Campana, F.W.B. Einstein, T. Jones, D. Sutton and A.S. Tracey, Inorg. Chem., 23 (1984) 363.

23 (a) B.J. Bruker, B.D. Santarsiero, M.S. Trimmer and J.E. Bercaw, J. Am. Chem. Soc., 110 (1988) 3134; (b) N.M. Doherty and J.E. Bercaw, J. Am. Chem. Soc., 107 (1985) 2670; (c) S.L. Buchwald and R.B. Nielsen, J. Am. Chem. Soc., 110 (1988) 3171.

24 (a) G. Chandra, A.D. Jenkins, M.F. Lappert and R.C. Srivastava, J. Chem. Soc. A, (1970) 2550; (b) M.H. Chisholm and M.W. Extine, J. Am. Chem. Soc., 99 (1977) 782; (c) M.H. Chisholm and M.W. Extine, J. Am. Chem. Soc., 99 (1977) 792.

25 (a) D.R. Walther, R. Mahrwald, C. Jahn and W. Klar, Z. Anorg. Chem., 423 (1976) 144; (b) E.C. Alyea, D.C. Bradley, M.F. Lappert and A.R. Sanger, J. Chem. Soc., Chem. Commun., (1969) 1064; (c) D.C. Bradley and M.H. Gitlitz, J. Chem. Soc. A, (1969) 1152; (d) D.C. Bradley and M.H. Gitlitz, J. Chem. Soc., Chem. Commun., (1965) 1289; (e) G. Chandra and M.F. Lappert, Inorg. Nucl. Chem. Lett., 1 (1965) 83.

26 M.F. Lappert and A.R. Sanger, J. Chem. Soc. A, (1971) 1314.

27 (a) B. Swanson and D.F. Shriver, Inorg. Chem., 9 (1970) 1406; (b) D.F. Shriver and B. Swanson, Inorg. Chem. 10 (1971) 1354.

28 R.E. Clarke and P.C. Ford, Inorg. Chem., 9 (1970) 227.

29 (a) P.M. Treichel, Adv. Organomet. Chem., 11 (1973) 21; (b) F. Bonati and G. Minghetti, Inorg. Chim. Acta, 9 (1974) 95.

30 (a) J.M. Manriquez, D.R. McAlister, R.D. Sanner and J.E. Bercaw, J. Am. Chem. Soc., 98 (1976) 6733; (b) J.M. Manriquez, D.R. McAlister, R.D. Sanner and J.E. Bercaw, J. Am. Chem. Soc., 100 (1978) 2716.
31 S.G. Davies (Ed.), Organotransition Metal Chemistry; Applications to Organic Synthesis, Pergamon Press, New York, 1983.
32 J.E. Hill, P.E. Fanwick and I.P. Rothwell, Organometallics, 9 (199) 2211.
33 G. Fachinetti, G. Fochi and C. Floriani, J. Organomet. Chem., 57 (173) C51
34 G. Fochi, C. Floriani, J.C.J. Bart and G. Giunchi, J. Chem. Soc., Dalton Trans., (1983) 1515 and references therein.
35 We have found that the reaction of $Cp_2Zr(CO)_2$ or $Cp_2Zr(PMe_2Ph)_2$ with azobenzene led only to intractable products in each case.
36 (a) A. Nakamura, M. Aotake and S. Otsuka, J. Am. Chem. Soc., 96 (1974) 3456; (b) S. Otsuka, A. Nakamura and H. Minamida, J. Chem. Soc., Chem. Commun., (1969) 1148.
37 J.C. Bart, I.W. Bassi, F. Cerruti and M. Calcaterra, Gazz. Chim. Ital., 110 (1980) 423.
38 R.S. Dickson and J.A. Ibers, J. Am. Chem. Soc., 94 (1972) 2988.
39 S.D. Ittel and J.A. Ibers, J. Organomet. Chem., 57 (1973) 389.
40 L.D. Durfree, J.E. Hill, P.E. Fanwick and I.P. Rothwell, Organometallics, 9 (1990) 75.
41 M.D. Fryzuk, T.S. Haddad and S.J. Rettig, J. Am. Chem. Soc., 112 (1990) 8185.
42 A. Mostad and C. Rømming, Acta Chim. Scand., 25 (1971) 3561.
43 R.G. Bergman, J.M. Buchanan, W.D. McGhee, R.A. Periana, P.F. Seidler, M.K. Trost and T.T. Wenzel, in A.L. Wayda and M.Y. Darensbourg (Eds.), Experimental Organometallic Chemistry: A Practicum in Synthesis and Characterization; ACS Symposium Series 357; American Chemical Society; Washington, DC, 1987, p. 227.
44 For a description of the X-ray diffraction and analysis protocols used see: (a) W.H. Hersh, F.J. Hollander and R.G. Bergman, J. Am. Chem. Soc., 105 (1983) 5834; (b) R.B. Roof Jr., "A Theoretical Extension of Reduced-Cell Concepts in Crystallography" Publication LA-4038, Los Alamos Scientific Laboratory: Los Alamos, NM 1969; (c) D.T. Cromer and J.T. Waber, International Tables for X-ray Crystallography": Kynoch Press: Birmingham, England, 1974; Vol. IV, Table 2.2B.